

1. Introduction

The techniques of multiple access in the Orthogonal Frequency Division Multiplexing (OFDM) system is always a popular and challenging topic. There are several types of multiple access techniques which could be applied to the OFDM system. The examples are OFDM-TDMA [1], OFDM-FDMA [2], and Multi Carrier-CDMA [3]. Except for the above methods, the character of the OFDM system provides a unique access capability: it can assign the specific subcarriers to the subscribers. This approach is called Orthogonal Frequency Division Multiple Access (OFDMA) [4]. OFDMA had been adopted as the physical layer multiple access technology in the standards such as IEEE 802.16e wireless Metropolitan Area Network (MAN).

Since the OFDMA system combines the OFDM system with the multiple access technique, it also comes with the drawbacks of the OFDM system. The OFDM system is highly sensitive to the carrier frequency offset. The Carrier Frequency Offset (CFO) is usually caused by the local oscillator synchronization error and / or the Doppler shift, resulting from the relative movement between the transmitter and the receiver. The CFO will introduce the loss of orthogonality (among subcarriers) so that the Inter-Carrier Interference (ICI) is produced. In OFDMA, the CFO further introduces Multiple Access Interference (MAI) and degrades the system performance [5]. Particularly in the uplink of the OFDMA systems, this problem becomes complicated because each user has a different CFO. The received signals are contaminated by the interference originated from subcarriers and users. Even if the correct synchronization occurs for the specific user, the transmitted information will not be correctly decoded in the base station. That is because the MAI from the other users is still not eliminated. Therefore, the mitigation of the synchronization error is a critical task in designing a

good OFDMA uplink receiver.

In the OFDMA uplink systems, the CFO and the Channel State Information (CSI) can be estimated [6] [7] [8]. This information can be used to avoid the ICI caused by the CFO. A way of solving the CFO problem is to inform all the mobile users their CFO information. Each individual mobile user can adjust the transmission signal to reduce the CFO. However, the feedback operation increases the system overhead and lowers the system throughput. To provide high performance for the OFDMA systems, alternative methods are required to solve the ICI and the MAI problems. In this thesis, we attempt to propose effective ICI and MAI cancellation algorithms for the uplink of OFDMA systems.

Two interference cancellation schemes are considered in this thesis. They are the Block Parallel Interference Cancellation (BPIC) and the Block Successive Interference Cancellation (BSIC). Both of these schemes are based on the Interference Cancellation (IC) principle [24], which is widely used for Multi-User Detection (MUD) in the CDMA system. The methods of BPIC and BSIC provide a good trade-off between the complexity and the performance. Besides, the usage of the random block assignment scheme to the subcarriers can not only take advantage of frequency diversity but has a good organization of its math model. Moreover, BPIC and BSIC can be implemented with multistage structures so that they can give the flexibility to meet all the system needs.

In this thesis, BPIC and BSIC are applied to the OFDMA system, in which we assume that the frequency offset and CSI were already known.

1.1. Motivation

The performance of OFDMA systems is sensitive to the carrier frequency offset, which is mainly caused by the synchronization error of the oscillators in the terminal and the base station sides. Especially in the uplink, the base station faces different CFOs from multiple subscribers. Due to the multiple access characteristic, it is difficult for the base station to synchronize all the subscribers' carrier frequencies at the same time. Without accurately estimating subscribers' carrier frequencies at the base station, the interference (MAI) from other subscribers always exists. This CFO problem in the multiple access system cannot be effectively solved by using the time domain approach. Therefore we focus the algorithms based on the frequency domain. In [23], the author applies the SIC structure to the OFDMA system. The system processes CFO in the frequency domain, and the structure he proposed is based on Single User Detector (SUD). It consumes lots complexity. Hence, we proposed another structure and cancellation algorithms to solve this problem.

We propose the BPIC and BSIC algorithms based on the information of CFO and CSI to solve the problem of the CFOs in the OFDMA uplink receiver.

1.2. Organization

This thesis will focus on the solutions of the interference caused by the CFO in the OFDMA. We will propose two new IC schemes to deal with this CFO problem. In this thesis, first, we will give the overviews of the OFDM and OFDMA systems in sections 1.3 and 1.4, respectively. In chapter 2, we concentrate on the CFOs problems of the OFDM and OFDMA systems. We start with mathematical model of the CFO in the single-user OFDM system and introduce the well-recognized approaches of solving the CFO problem. Then, base on fundamental model for the CFO in the OFDM system, we build the OFDMA signal model with CFOs. Finally, we introduce

the previously published methods proposed to solve the problem. In chapter 3, we will propose the block based interference cancellation schemes: Block Parallel Interference Cancellation (BPIC) and Block Successive Interference Cancellation (BSIC). In chapter 4, we show the computer simulation results and make the performance evaluation of the proposed methods and the previously proposed methods. In Chapter 5, we will give a conclusion and discuss the future work of the OFDMA system.

1.3. Overview of the OFDM System

Unlike the traditional single carrier modulation system, the OFDM system transmits data by using multiple subcarriers (let N be the number of subcarriers), which are orthogonal to each other. Due to the parallel transmission, the symbol time is extended to N times of the origin. The OFDM is a special kind of Frequency Division Multiplexing (FDM) technique. By use of FFT/IFFT and the cyclic prefix/postfix, the subcarriers are orthogonal to each other. The equalization can be easily performed in the frequency domain.

Normally in the FDM-type system, guard bands in frequency domain are used to prevent the interference caused by the adjacent carriers. However, the OFDM system does not need guard band because of the orthogonality between the subcarriers. In other words, the OFDM has higher spectral usage efficiency than the FDM [9]. That is why the OFDM is attractive in the broadband communication systems. Figure 1.3.0.1 illustrates an example of frequency usage between the traditional FDM and OFDM. Apparently, OFDM saves about 50 % of the original bandwidth while sending the same information as the FDM.

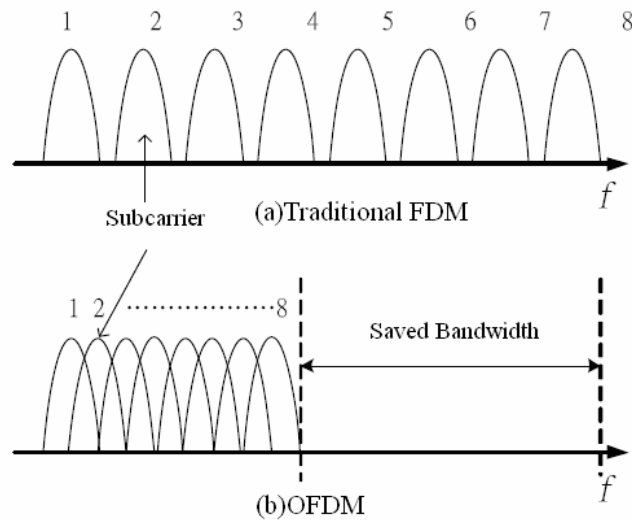


Figure 1.3.0.1 Spectrum of FDM and OFDM

The idea of transmitting parallel data with FDM was brought out in mid 1960s [10]. The original purposes were to prevent the usage of a complex high speed equalizer and reduce multi-path fading. However, the Digital Signal Process (DSP) technique was not well developed at that time. It was complicated and costly to implement an orthogonal signal generator and the filters. This technique was not paid much attention until the idea of replacing the analog multi-carriers generator with the Inverse Fast Fourier Transform (IFFT) and Fast Fourier Transform (FFT). Another important OFDM technique was brought out in 1980 by Peled and Ruiz to utilize the cyclic extension. The cyclic extension can solve the distortion of orthogonality between subcarriers produced by IFFT and FFT.

Nowadays the OFDM technique is broadly applied to communication systems. It is used in the wired communication, such as HDSL(High-bit-rate Digital Subscriber Loop) 、ADSL(Asymmetric DSL) and VDSL(Very-high-speed DSL), and also in wireless communication, such as DAB (Digital Audio Broadcasting) and DVB (Digital Video Broadcasting).

1.3.1 OFDM Signal Characteristics

The basic concept of OFDM is to modulate the original signals into the different orthogonal subcarriers. The symbol duration is the multiples of the single carrier symbol period. Figure 1.3.1.1 ($n=3$) shows an example of the OFDM signal concept. In the figure, there are three subcarriers for parallel transmission, and the symbol duration is three times of the single carrier.

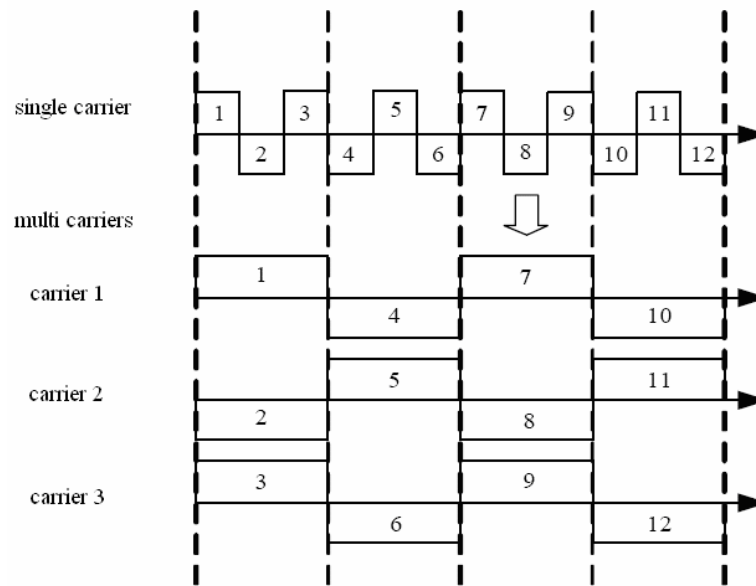


Figure 1.3.1.1 OFDM signal concept

In the rest of this chapter, we will have a brief introduction of the digital implement of OFDM system.

A. Modulation of the OFDM system

The OFDM signal is described as follows, where $s(t)$ is the analog OFDM signal:

$$s[n] = s(t) |_{t=nT_d} = \begin{cases} \frac{1}{\sqrt{N}} \sum_{k=-N/2}^{N/2} X_k e^{j2\pi \frac{k}{N} n} & , 0 \leq n \leq N - 1 = IFFT\{X_k\} \\ 0 & , \text{otherwise} \end{cases} \quad (1.1)$$

X_k is the transmitted symbol (M -PSK or M -QAM), T_d is the sampling period, and $T_d = T / N$ where T is the symbol duration.

Figure 1.3.1.2 shows the structure of the discrete-time OFDM modulation system. Input symbols are sent to the Serial to Parallel (S/P) converter and then modulated by the IFFT. The IFFT modulation transforms the data from frequency domain to time domain. The Parallel to Serial (P/S) converter combines the parallel digital data into a data stream $s[n]$. Finally, the Digital to Analog (D/A) converter builds the ideal analog OFDM baseband signal $s(t)$.

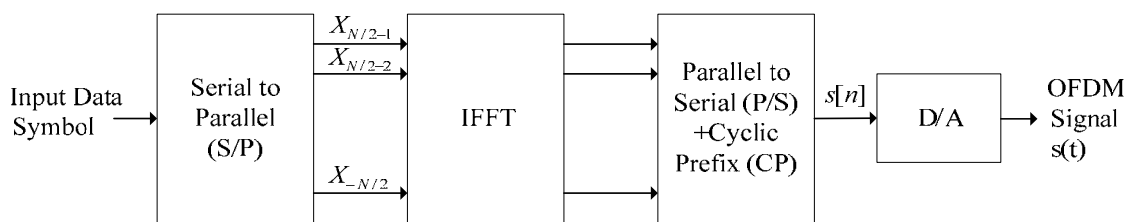


Figure 1.3.1.2 Discrete-time OFDM modulation system

B. Demodulation of OFDM system

The baseband OFDM receiver's operations are the inverse of the transmitter's, and the inverse of IFFT is FFT. Therefore, the base band receiver can be easily implemented by FFT. In figure 1.3.1.3, the received OFDM signal $r(t)$ was input into the A/D converter. Then, the sampled digital stream data, $r[n]$, are converted from series to parallel by the S/P converter. The FFT transforms the data from the time domain to the frequency domain.

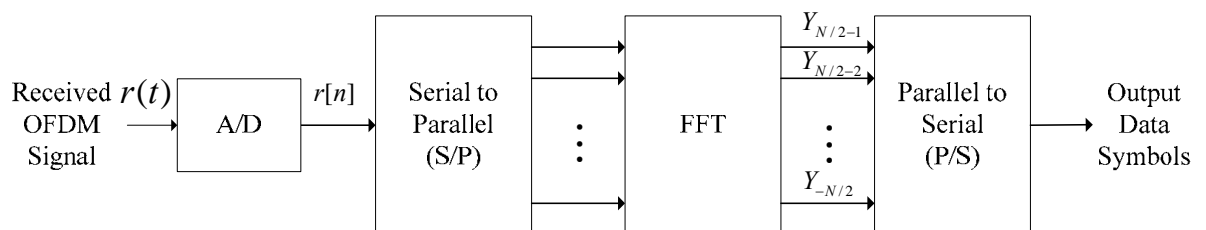


Figure 1.3.1.3 Discrete-time OFDM demodulation system

$$Y_h = \begin{cases} \frac{1}{\sqrt{N}} \sum_{n=-N/2}^{N/2} r[n] e^{-j2\pi \frac{h}{N} n}, & 0 \leq n \leq N-1 = FFT\{r[n]\} \\ 0, & \text{otherwise} \end{cases} \quad (1.2)$$

1.3.2 Guard Interval and Cyclic Prefix

In the multi-path channel, the delayed replicas of previous OFDM signal can lead to an Inter-Symbol Interference (ISI). To eliminate the interference in the OFDM system, we may add a period of silent guard interval into each OFDM block, like figure 1.3.2.1. The added guard interval should be longer than the maximum delay spread so that the previous delayed block of OFDM signal will not interfere the next block.

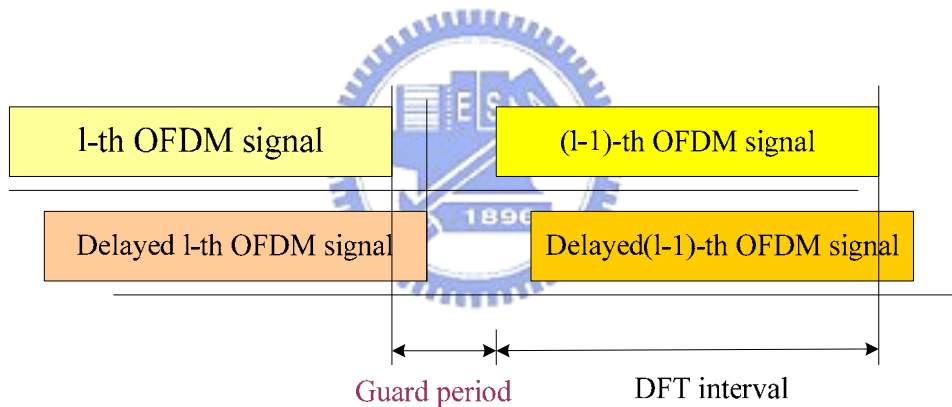


Figure 1.3.2.1 Silence Guard interval

However, the silent guard interval will lead to an Inter-Carrier Interference (ICI) in the OFDM demodulation. In figure 1.3.2.2, the subcarriers have different delay spreads. The silent guard interval breaks the orthogonality after FFT demodulation.

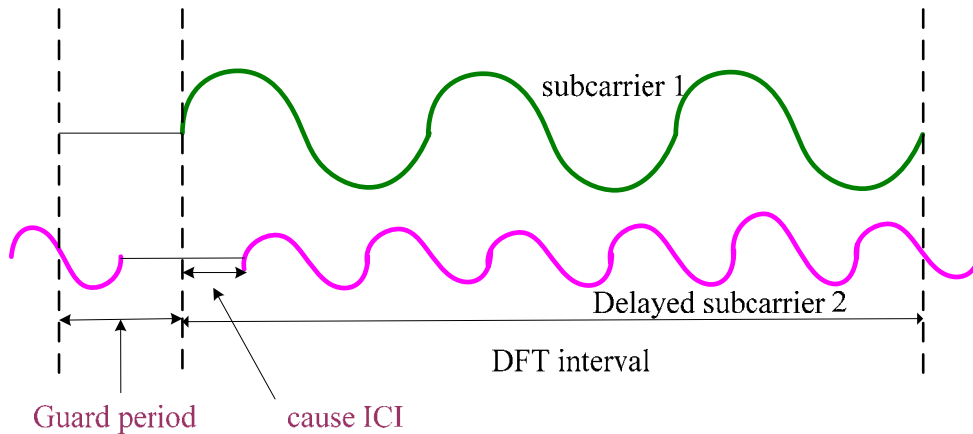


Figure 1.3.2.2 ICI caused by silent guard interval with delay spread

In order to keep the orthogonality and diminish the influence of multi-path, the Cyclic Prefix (CP) is applied. The CP is a copy of the last part of OFDM signal, which is attached to the front of itself.

Figure 1.3.2.3 is the structure of the complete OFDM signal with the CP. N_g is the length of the CP, and N is the size of FFT and IFFT. After attaching the last N_g symbols, the total length of OFDM signal becomes $N_g + N$.

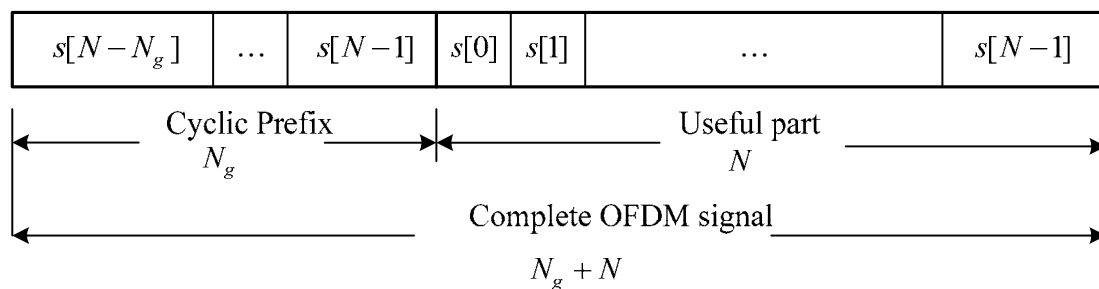


Figure 1.3.2.3 The structure of the complete OFDM signal with Cyclic Prefix

Figure 1.3.2.4 shows the complete OFDM transmitter and receiver. We add the guard interval with CP in the P/S converter of the transmitter and remove the guard interval after the A/D converter in the receiver.

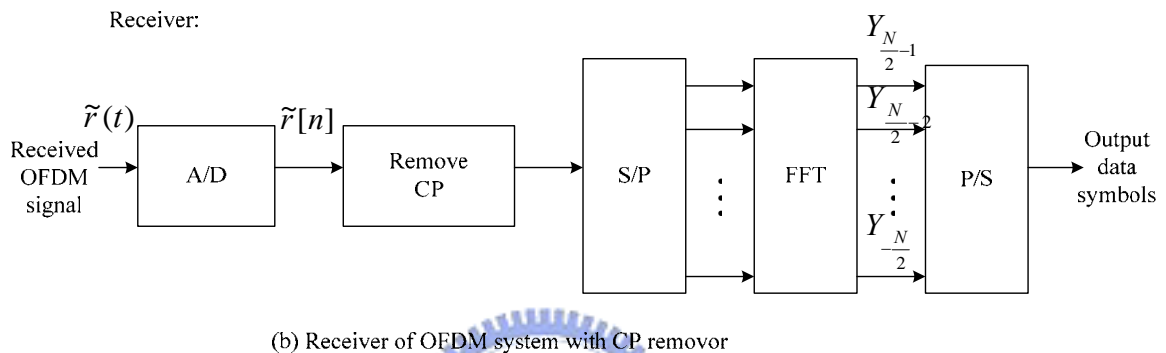
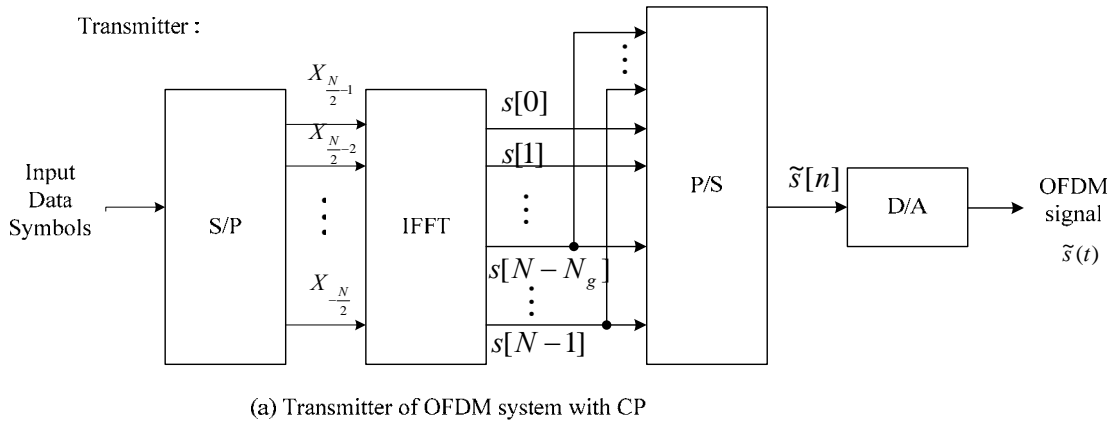


Figure 1.3.2.4 (a) OFDM Transmitter (b) OFDM Receiver

To summarize, the advantages of OFDM system are as follow:

- The spectral usage of the OFDM system is more efficient than the traditional FDM system.
- The OFDM system is robust to the interference caused by multi-paths As long as the maximum delay spread is less than the CP, the frequency domain equalizer can successfully solve the multi-path problem.
- Compared to the narrowband system, the OFDM system can take advantage of the frequency diversity.

The disadvantages of the OFDM system are:

- The OFDM system is sensitive to the frequency errors and the phase noise.
- The Peak to Average Power Ratio (PAPR) problem may cause non-linear

distortion, increase the design complexity of power amplifier, and roll back the power efficiency.

1.4. Overview of the OFDMA System

The OFDMA is a multiplex technique. The subcarriers are grouped into several subchannels, and these subchannels are allocated to the multiple users for the concurrent transmission. The orthogonality among the subcarriers can eliminate each user's ISI and MAI.

Moreover, Frequency Hopping (FH) technique can be employed into the OFDMA system and form an FH-OFDMA system. The advantages of FH-OFDMA are well known in [16][17] and [18]. If the channel frequency response varies over the hopping distance, the frequency diversity can be obtained through coding. The interference diversity can even be achieved, while the decoder metrics are properly weighted according to the interference power encountered in each hop. Therefore, the technique of FH improves the performance and gives high frequency re-usage. In this thesis we will focused on the problem of CFO. The hopping algorithm will not be discussed.

In the following subsections, the architectures of the OFDMA system will be introduced. The signal model of the proposed OFDMA system will be discussed.

1.4.1 Architectures of the OFDMA System

A. Single User Detector based (SUD) OFDMA system

The SUD OFDMA multiuser receiver is composed of numbers of single user receivers. At the transmitter, the subscriber transmits signal by the use of the assigned subcarriers, and the unused subcarriers are sending null data. The subcarriers of the different subcarriers are not overlapped.

Assume that U is the number of the total subscribers, N is the size of IFFT and FFT, f_c is the carrier frequency of the multiuser receiver, and Δf_i represents the CFO of the i -th subscriber. Figure 1.4.1.1 (a) shows the OFDMA UP-Link transmitter structure. With the proper assignment of subcarriers and hopping rules, it can achieve the frequency diversity. Figure 1.4.1.1 (b) shows that the receiver of base station is made up of several single user detectors. After the A/D converter, the CFOs are compensated in time domain according to their frequency estimation, and then the signals are fed into the size N FFT for demodulation.

Because each path needs N point FFT to demodulate its own signal, the computation and complexity are high. In addition, the compensation in time domain can not completely eliminate the interference.

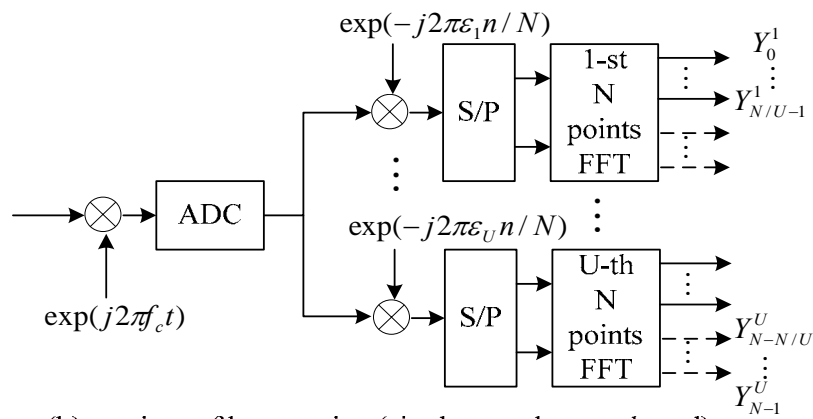
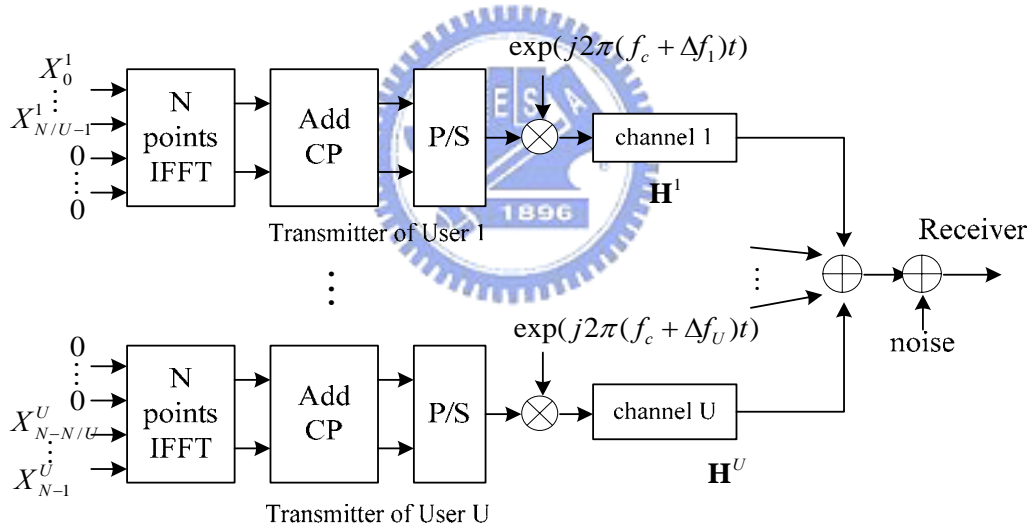


Figure 1.4.1.1 (a) Transmitters and channels in uplink of OFDMA

(b) Receiver of based station (single user based)

B. Poly-Phase Filter Bank based (PPFB) OFDMA system

The PPFB OFDMA structure is based on the filter bank. The filter bank is employed in the multiuser receiver to separate the signals of different users. From [19] [20], the PPFB structure is able to effectively decrease MAI and separate the overlapped multiuser's signals with insertion of a guard frequency. The PPFB is a Filtered Multi-tone Transmission (FMT) system. Though the PPFB system adopts the guard band to reduce the interference, it still comes with the drawbacks of FMT systems. First, the FMT system is sensitive to the multi-path delay spread in frequency selective radio channel. Second, the FMT system with large number of subcarriers, say, 2048 is prohibitively complicated. Third, the FMT system with large transition bands has poor spectrum efficiency. Moreover, the prototype filter [19] in the PPFB is hard to be implemented. It needs filters with 320 taps.

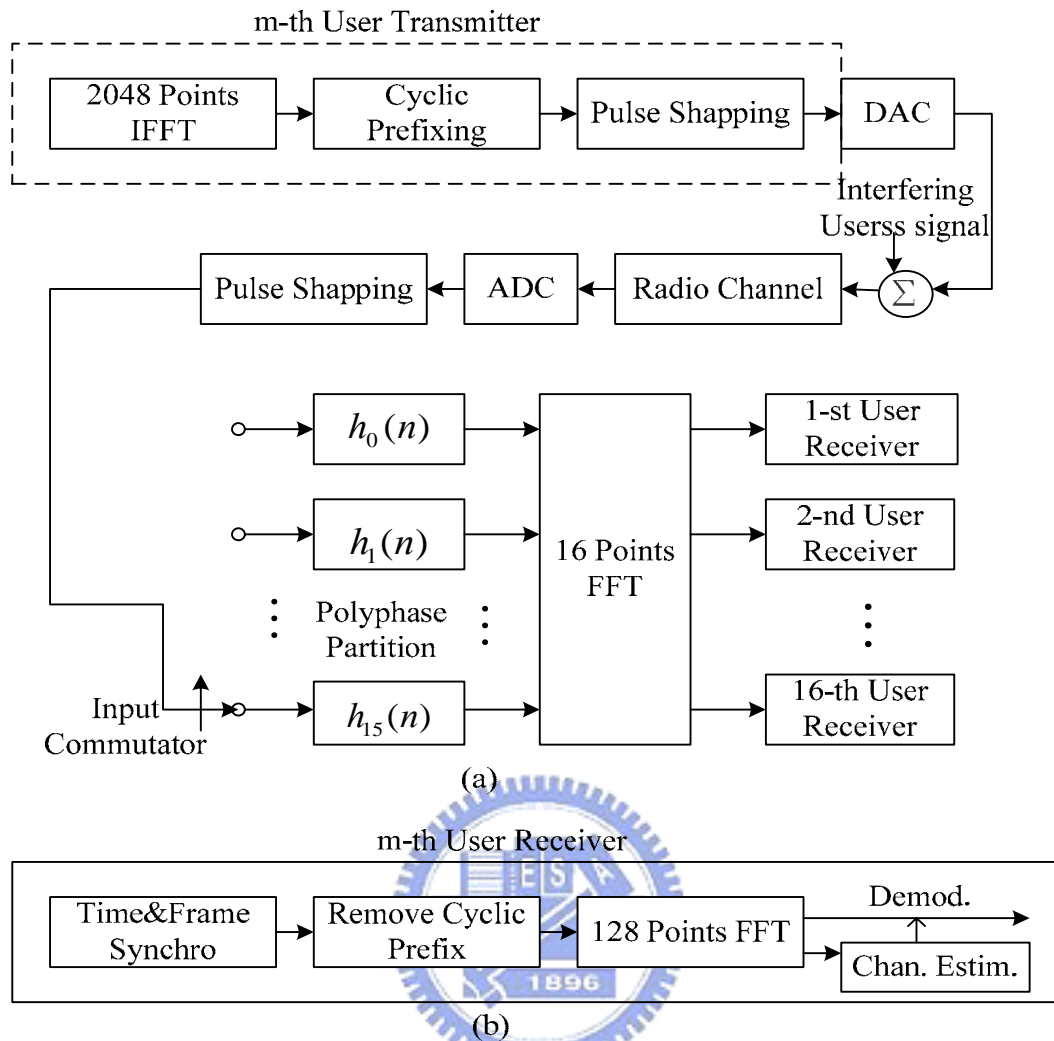


Figure 1.4.1.2 Block diagram of the filter bank OFDMA system.

At the receiver side, the input commutator does sample rate reduction by commutating successive input samples to the selected paths of 16-path filter. The band pass signal is transformed to baseband by down sampling. The prototype filter $h_m(n)$ is employed to shape the baseband signal in the m -th channel ployphase partition. Note that the functions of FFT between transmitter and receiver are different. The 2048 points FFT at the transmitter is acted as the modulator. The first 16 points FFT at the receiver is for channel separation. Only the last 128 points FFT are employed in demodulation for one user. The computation in FFT part of PPFB does save a lot and draw much attraction.

C. Proposed OFDMA system

The proposed OFDMA system is a block based OFDMA system. The system partitions the total subcarriers into several block units, and each block has the successive subcarriers. In other words, each subscriber is allocated with a block of subcarriers.

The block based OFDMA system can also take advantage of the frequency diversity by the random block assignment. While facing the frequency selective channel, the system may permute the sequence of the used blocks. This will disperse the illness from the block with worse channel frequency response. Moreover, the block based OFDMA system can be easily modeled and has nice mathematical characteristics. We can make use of these for the interference cancellation.

Assume that N is the size of FFT and IFFT, and U is the number of subscribers. We fairly separate the total N subcarriers into size of N/U as a block in the figure 1.4.1.3.

Comparing the proposed scheme with SUD-based one, the block based OFDMA multi-user receiver requires an N -point FFT instead of multiple FFTs. This saves tremendous computation.

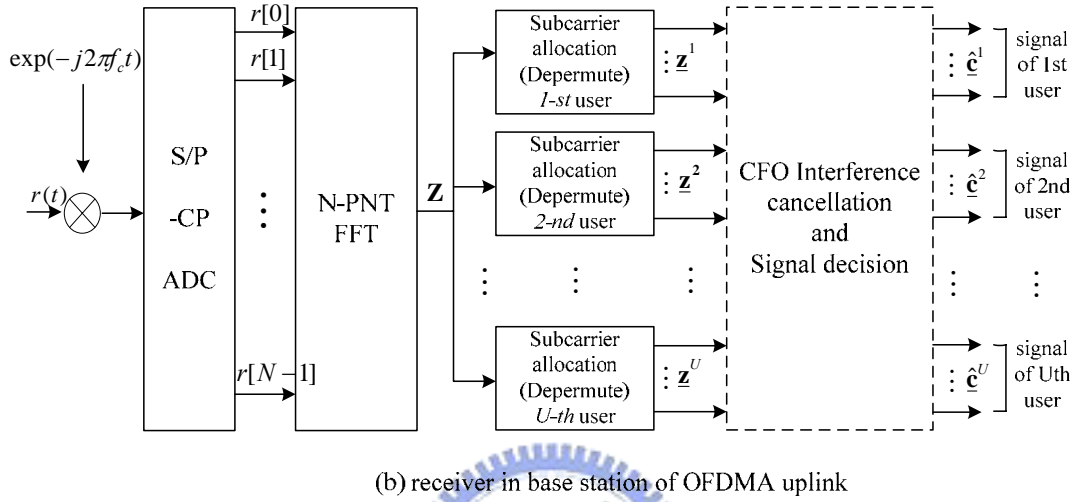
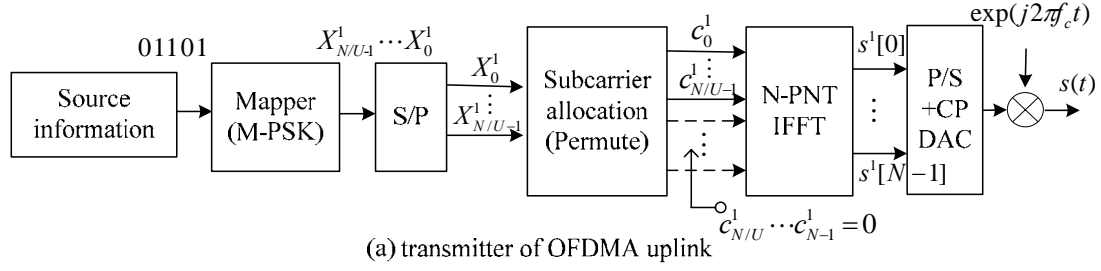


Figure 1.4.1.3 Block diagram of uplink proposed OFDM system

1.4.2 The OFDMA Signal Model of the Proposed Architecture

In this section, the OFDMA signal will be analyzed in the view of ideal uplink transmission without the CFO interference.

A. Modulation of OFDMA system (SS)

We take the m -th subscriber as an example, the source information is mapped into M-PSK: X_k^m , where $k = 0, \dots, N/U$, N is the total number of system subscribers, and U is the number of subscribers. After the S/P conversion, the parallel signals were input into the subcarrier allocation device. For the purpose of easy comprehension, we discuss the functionality of the devices and the flow of signals as follows:

- ◆ Original M-PSK signal after S/P: $\mathbf{X}^m = [X_0^m, \dots, X_{N/U-1}^m]^T, N/U \times 1$. The original transmitted data were mapped into high modulation. Assume the

system fairly partitions the total available subcarriers N into N/U , and the subscriber transmits in the unit of block.

- ◆ Subcarriers allocation:

$$\mathbf{c}^m = \mathbf{T}^m \mathbf{X}^m = [0, \dots, 0, X_0^m, \dots, X_{N/U-1}^m, 0, \dots, 0]^T = [c_0^m, \dots, c_{N-1}^m]^T, N \times 1. \quad (1.3)$$

The permutation behavior can be modeled in an $(N \times N/U)$ permutation matrix: \mathbf{T}^m , which permutes the block of N/U subcarriers into assigned location and extend the size to N .

The purpose of the subcarrier allocation device is to interleave the block of subscriber and take advantage of frequency diversity.

- ◆ Signal after N-point IFFT modulation:

$$s^m[n] = \sum_{l=0}^{N-1} c_l^m e^{j2\pi nl/N}. \quad (1.4)$$

The signals are modulated to time domain by IFFT and then attached cyclic prefix (CP) for conquering the channel delay spread.

- ◆ The signal after DAC is modulated with carrier frequency: $s^m(t) \exp(j2\pi f_c t)$ to RF.

B. Demodulation of OFDMA system (BS)

At the multiuser receiver of the base station, the received signal is the sum of signals from different subscribers and the channel noise. Herein, assume there is no difference or offset carrier frequencies of Tx and Rx.. In others words, the CFO is zero. We discuss the functionality of the device and the flow of the signals as follows:

- ◆ RF signal received at the base station:

$$r(t) \exp(-j2\pi f_c t) = \sum_{i=0}^{U-1} r^i(t) \exp(-j2\pi f_c^i t) + noise \quad (1.5)$$

$$r^i(t) = s^i(t) * h^i(t) + n^i(t)$$

$r(t)$ is the sum of received RF signal with noise, and $r^i(t)$ is the i -th subscriber's signal. It is a convolution of the transmitted signal and the

channel impulse response $h^i(t)$. $n^i(t)$ is the AWGN noise with power $N_0/2$.

At the RF end, the signal will be demodulated into the baseband by using the estimated carrier frequency. By the assumption before, the estimated frequency is f_c and $f_c = f_c^i, i=1, \dots, U$.

- ◆ The based band CFO free signal after sampling:

$$\mathbf{r} = [r[0], r[1], \dots, r[N-1]]^T, N \times 1, \text{ where } r[n] = \sum_{i=0}^{U-1} r^i[n] \quad (1.6)$$

All users are assumed to be synchronized in time domain. By the advantage of CP, the convolution between $s^i(t)$ and $h^i(t)$ is a cyclic convolution. The i -th received signal can be define as $r^i[n] = s^i[n] \otimes h^i[n] + n^i[n]$, $n^i[n]$ is AWGN noise contribution with power spectral density $N_0/2$.

- ◆ The signal is demodulated with N point FFT:

$$\mathbf{Z} = [z_0, z_1, \dots, z_{N-1}]^T, \text{ where } z_k = \frac{1}{N} \sum_{n=0}^{N-1} r[n] e^{-j \frac{2\pi}{N} nk} = \frac{1}{N} \sum_{i=0}^{U-1} \sum_{l=0}^{N-1} H_l^i c_l^i \sum_{n=0}^{N-1} e^{-j \frac{2\pi}{N} n(k-l)} + N_k \quad (1.7)$$

H_l^i is the channel impulse response of the i -th user at the l -th subcarrier in frequency domain. N_k is the noise term of the k -th subcarrier in frequency domain.

- ◆ Subcarriers allocation:

The subcarrier allocation performs the inverse operation as that in the transmitter. The device responses for the de-interleaving (de-permutation) and arranges the block signals back to its own location for the latter interference cancellation. To understand the operations, the figure 1.4.2.1 shows the block diagrams of inverse subcarrier allocation and the mathematical expression.

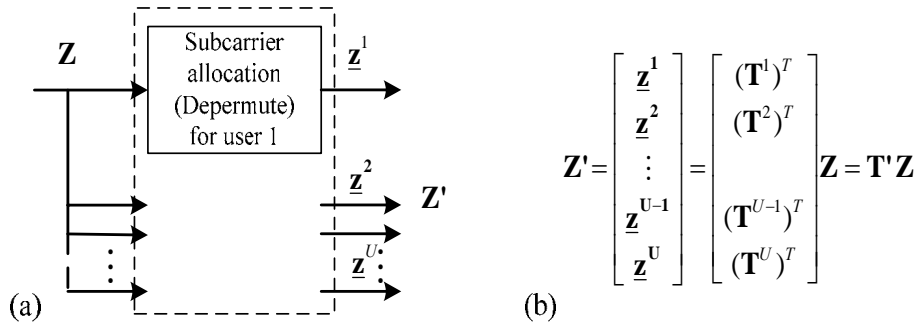


Figure 1.4.2.1 Block diagrams of de-permutation and its mathematical expression

The boldface text represents a vector or a matrix, the capital and boldface text is a total signal, and the lowercase and boldface means the cluster of signal. In mathematic, the de-permutation of the i -th user is to multiply a transpose of the permutation matrix. The dotted part in (a) can be modeled as a matrix, \mathbf{T}' , which is composed of cascaded submatrix $(\mathbf{T}^i)^T$.

The block based OFDMA system signal flow is shown above. Without any noise and under perfect channel transmission, the signal can be perfectly obtained after de-permuatation.

2. The Carrier Offset Problem in the OFDMA System

In this chapter, we will first discuss the phenomena of carrier frequency offset (CFO) under the systems of OFDM and OFDMA. Then we will introduce previously published methods of solving the CFOs problem.

2.1. Carrier Frequency Offset of OFDM system

The CFO is one of the important problems in the OFDM system. The innate frequency mismatch of the oscillators in the Tx and the Rx will induce the co-channel interference after FFT demodulation. The following figure 2.1.1 shows the concept of CFO.

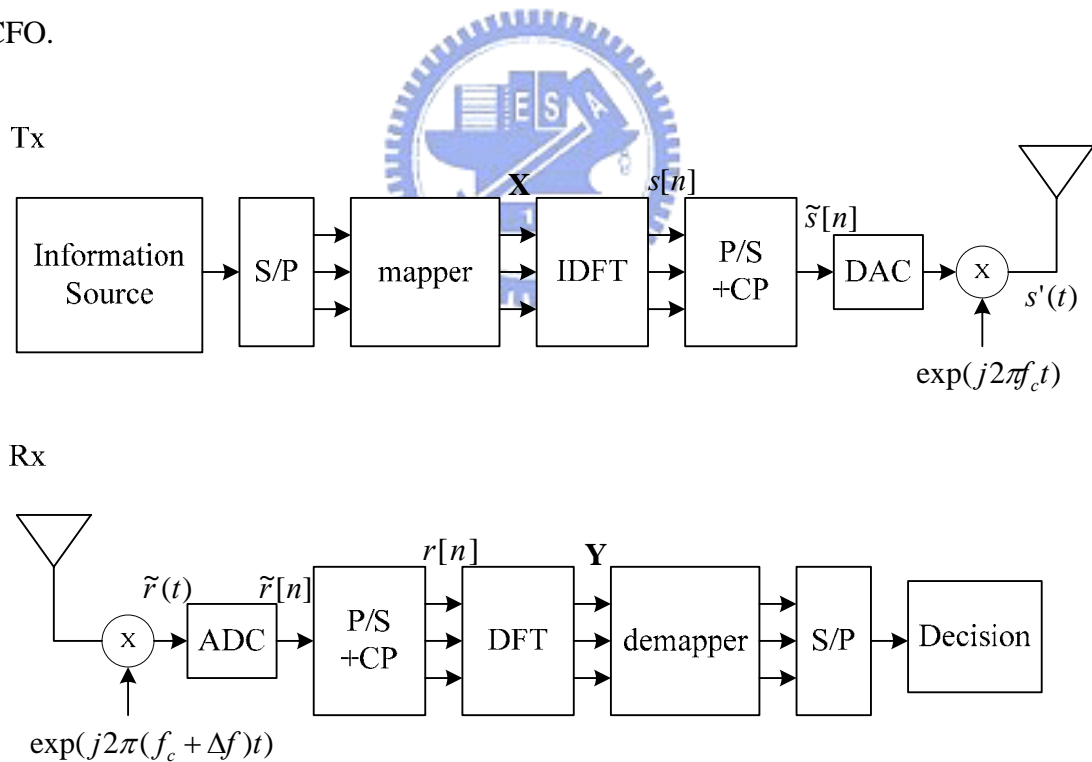


Figure 2.1.1 Carrier frequency offset between TX and RX

The CFO Δf ($\Delta f = f_{tx} - f_{rx}$) between the transmitter and the receiver oscillators can be expressed as a time-variant phase error, $e^{j2\pi\Delta f t}$. The signal after guard interval

removing can be expressed as:

$$r[n] = \frac{1}{N} e^{j2\pi n/N} \cdot \sum_{k=1}^{N-1} H_k X_k e^{j2\pi kn/N} + w[n], n = 0, 1, 2, \dots, N \quad (2.1)$$

Therein, $\varepsilon = \Delta f / f_{sub}$ denotes user relative CFO value, and f_{sub} is the frequency distance of adjacent subcarriers. H_k and X_k are user's channel state information (CSI) and the transmit data, respectively. $w[n]$ is the noise term.

After demodulating the received signal $r[n]$ by using DFT, the k -th symbol of subcarrier in frequency domain can be represented as:

$$\begin{aligned} Y_k &= \frac{1}{N} \sum_{n=0}^{N-1} r[n] e^{-j2\pi n(k+\varepsilon)/N} = \frac{1}{N} \cdot \frac{1}{N} \sum_{n=0}^{N-1} \left(\sum_{k=1}^{N-1} H_k X_k e^{j2\pi kn/N} + w[n] \right) e^{-j2\pi n(k+\varepsilon)/N} \\ &= I_{k,k} H_k X_k + \sum_{k'=0, k' \neq k}^{N-1} I_{k,k'} H_{k'} X_{k'} + w_k \end{aligned} \quad (2.2)$$

The first term in Eq. 2.2 is the desired signal with interference contributed by the symbol itself, the second term is ICI, and the third term is the noise term.

$$I_{k,k'} = \frac{1}{N} \sum_{n=0}^{N-1} e^{j2\pi n[(k'-k)+\varepsilon]/N} = \frac{\sin \pi(k'-k-\varepsilon)}{N \sin \frac{\pi}{N}(k'-k-\varepsilon)} \cdot e^{-j\pi(1-\frac{1}{N})(k'-k-\varepsilon)} \quad (2.3)$$

The equation 2.3 is the CFO interference term, which was contributed from the k' -th subcarrier to the k -th.

We can realize the CFO problem in other point of view. The DFT demodulation is to sample the signals in frequency domain. In addition, a time varying phase term, which was transformed into the frequency domain, will cause a shift in frequency domain. Therefore, the CFO problem makes a sampling point shift in frequency domain and breaks the orthogonality.

In the figure 2.1.2, you can observe the amplitude of interference term, $I_{k,k'}$, with

different degrees of CFO. We fix the index $k = 0$. The FFT size N is 8. The CFO values normalized to subcarrier space are $\varepsilon = 0.2$, $\varepsilon = 0.3$, and $\varepsilon = 0.4$. It is evident that when the CFO value becomes larger, the desired part $I_{k,k}$ decreases and the undesired part $I_{k,k'}, k' \neq k$ increases.

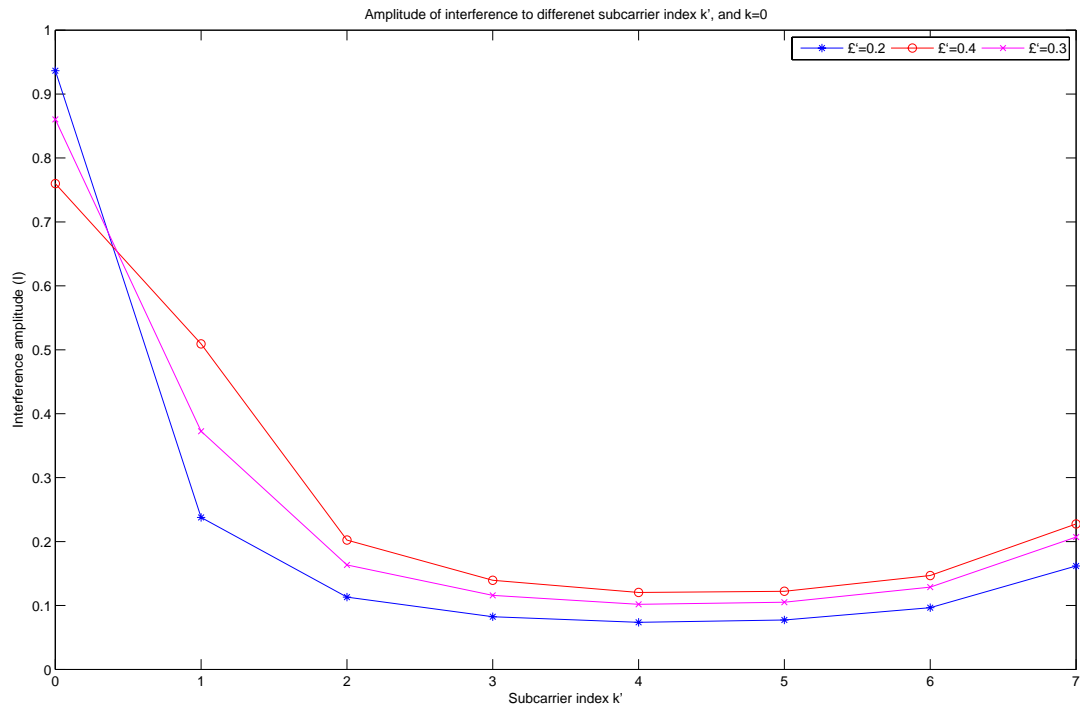


Figure 2.1.2 Amplitude of interference to difference carrier frequency offset

The signal $Y_k, k = 0, 1, \dots, N-1$ can be written into matrix form:

$\mathbf{Y} = [Y_0 \ \dots \ Y_{N-1}]^T$, and rewrite the equation (2.2) as:

$$\mathbf{Y} = \mathbf{H}\mathbf{X} + \mathbf{W} \quad (2.4)$$

$$\mathbf{H} = \begin{bmatrix} H_0 & 0 & \dots & 0 \\ 0 & \ddots & & \vdots \\ \vdots & & \ddots & 0 \\ 0 & \dots & 0 & H_{N-1} \end{bmatrix}$$

is the channel impulse response matrix in frequency

domain. $\mathbf{I} = \begin{bmatrix} I_{0,0} & I_{0,1} & \cdots & I_{0,N-1} \\ I_{1,0} & I_{1,1} & \cdots & I_{1,N-1} \\ \vdots & \vdots & & \vdots \\ I_{N-1,0} & I_{N-1,1} & \cdots & I_{N-1} \end{bmatrix}$ is the interference matrix, where the

diagonal entries are the desired signal scales, and the others are ICI components.

$\mathbf{X} = [X_0 \ \cdots \ X_{N-1}]^T$ is the transmitted data symbol, and $\mathbf{W} = [W_0 \ \cdots \ W_{N-1}]^T$ is

the noise term. The most interesting is that interference matrix \mathbf{I} becomes a Toeplitz matrix format, because every subcarrier was suffered the same CFO. Toeplitz matrix

\mathbf{I} is a matrix whose i, j th element $I_{i,j}$ is only function of the value $(i - j)$.

Therefore, it has identical elements along the main diagonal and subdiagonal.

Figure 2.1.3 has two graphics. In the graphic (a), the different color represents a different value, and you can tell that the interference matrix \mathbf{I} is a Toeplitz matrix.

The graphic (b) shows that the most significant values are always located in the diagonal elements. Besides, the most serious interference values happen in the adjacent subcarriers.

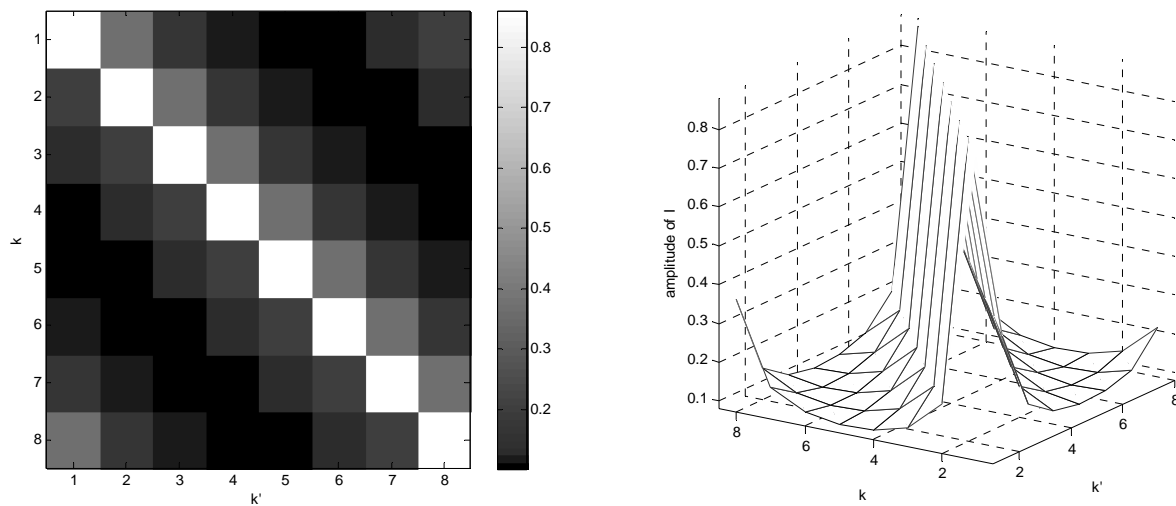


Figure 2.1.3 (a) The image of interference matrix in OFDM

(b) The mesh of interference matrix in OFDM

2.2. Methods of Reducing Interference due to Carrier Frequency

Offset

A number of methods have been developed to reduce the effects caused by the frequency offset. They can be separated into two groups. One group is the self ICI cancellation schemes, and the other is the windowing approach.

A. Self ICI Cancellation Schemes

Zhao and Haggman [11] have described a method of reducing the interference caused by frequency errors, It is called the self ICI cancellation. The method maps the transmitted data onto adjacent parts of subcarriers rather than onto single subcarrier, $X_0 = -X_1, X_2 = -X_3, \dots, X_{N-2} = -X_{N-1}$. It results in the cancellation of the most ICI in the values: Z_0, \dots, Z_{N-1} .


For example, the received signal on the l -th subcarrier becomes:

$$Z_l = \exp(j\theta_0) \sum_{\substack{k=0 \\ k=even}}^{N-2} X_k [I_{l,k} - I_{l+1,k}] + n_l \quad (2.5)$$

where θ_0 is the phase offset between the phase of the receiver local oscillator and the carrier phase at the start of the received symbol. In this case, the ICI coefficient is denoted as $I'_{l,k} = I_{l,k} - I_{l+1,k}$.

The ICI cancellation does not depend on the absolute values of the coefficients but their difference so that it can improve the performance for any frequency offset. However, it is less bandwidth efficient than the original OFDM. Only a half of the original data information can be transmitted per symbol.

B. Windowing

A number of authors have described the usage of windowing in the OFDM system. This method can be divided into two groups. One is about the Windowing to reduce the sitivity of linear distortions [12]. The other is about Windowing to

reduce the sensitivity of frequency offset [11][13]. The second group is what we care about.

The second group of windowing methods adds the cyclic extension by v samples. The resulting signal is then shaped with the window function. Figure 2.2.1 shows a block diagram of a typical windowing system. Note that the transform in the receiver is N point whereas that in the transmitter is $N/2$ point. The $N/2$ inputs to the transmitter transform have been labeled as $X_0, X_1, \dots, X_{N/2-1}$.

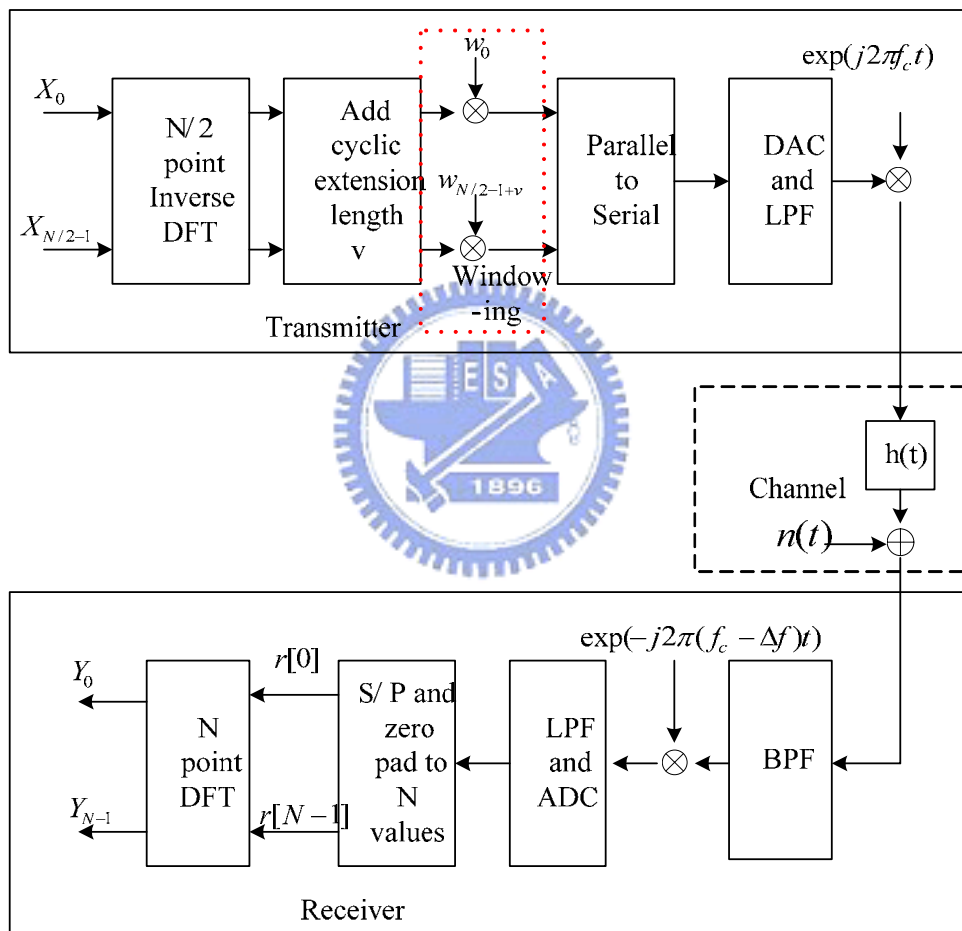


Figure 2.2.1 Windowing to reduce sensitivity to frequency offset

Because not the entire received signal power is used to generate the data estimates, the method has reduced overall Signal to Noise Ratio (SNR) in comparison with the OFDM system without windowing. The value of the SNR loss depends on

the form of windowing.

A number of different windows, including the Hanning window [14], the windows satisfying the Nyquist criterion [15], and the Kaiser window, have described in the literature [15]. All these windows give some reduction of the sensitivity to frequency offset. But only the Nyquist windows (of which the Hanning window is one particular example) have no ICI for the case without frequency offset [15].

2.3. Carrier Frequency Offset of OFDMA System

One of the challenging tasks in the OFDMA system is the CFOs problem at multiuser receiver in the base station. People know that the major reason of CFOs is the misalignment between the oscillator frequencies of TX and RX. However, the OFDMA is a multiple access system; in the uplink, the receiver at the base station has various CFOs from different subscribers as shown in figure 2.3.1. Let Δf^i denote the CFO of the i -th subscriber.

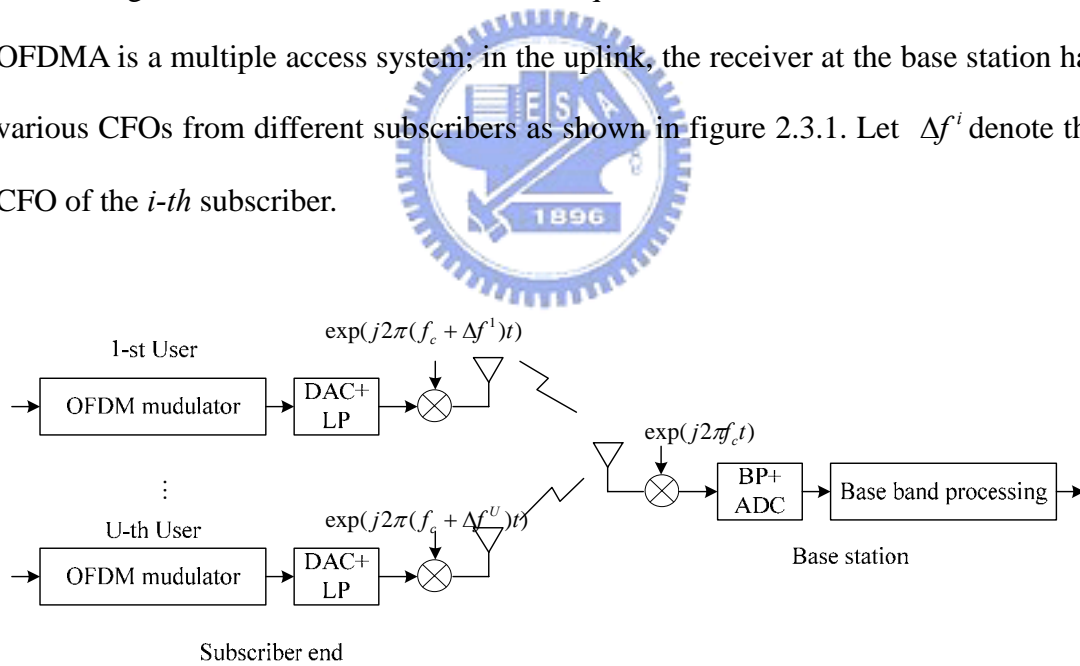


Figure 2.3.1 Concept of CFO in OFDMA uplink

For easy comprehension, the OFDMA system with CFOs can be simplified into the form as shown in figure 2.3.2.

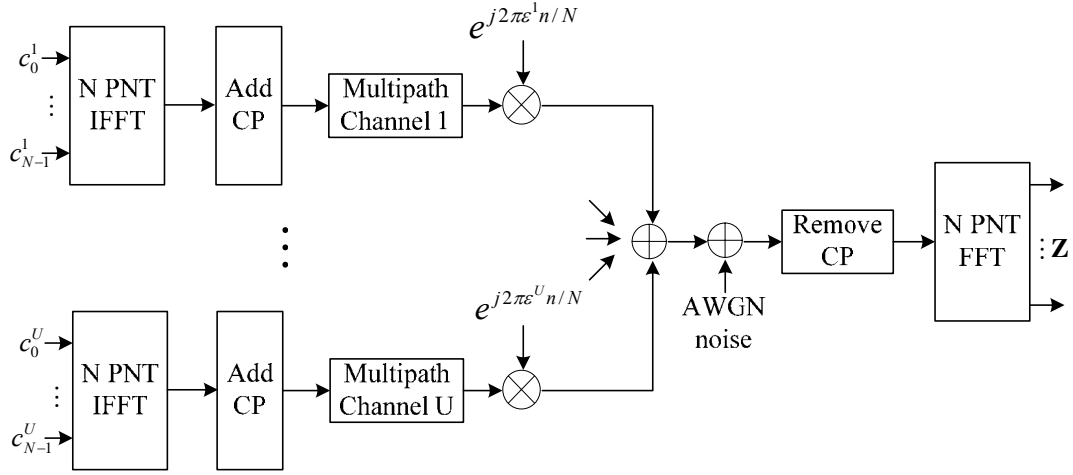


Figure 2.3.2 Simplified OFDMA uplink system with CFOs

Base on the description in the last section, $\mathbf{c}^i = [c_0^i, c_1^i, \dots, c_{N-1}^i]^T$ is the block of N symbols, which were extended by permutation of the original block of N/U symbols, \mathbf{X}^i . Therein $\epsilon^i = \Delta f^i / f_{sub}$ denotes the i -th user's relative CFO value, f_{sub} is the spacing between two adjacent subcarriers, and Δf^i is the absolute CFO of the i -th user.

The IFFT output for the k -th subcarrier which belongs to the j -th user becomes:

$$\begin{aligned} z_k^j &= \frac{1}{N} \sum_{n=0}^{N-1} r[n] e^{-\frac{j2\pi nk}{N}} = \frac{1}{N} \sum_{i=0}^{U-1} \sum_{l=0}^{N-1} H_l^i c_l^i \sum_{n=0}^{N-1} e^{(-\frac{2\pi}{N}n(k-l-\epsilon^i))} + N_k \\ &= \sum_{i=0}^{U-1} \sum_{l=0}^{N-1} I_{l-k}^i H_l^i c_l^i + N_k \end{aligned} \quad (2.7)$$

Herein, H_l^i is the sample of channel impulse response of the i -th user and the l -th subcarrier in the frequency domain.

$$I_{k-l}^i = \frac{\sin \pi(k-l-\delta^i)}{N \sin \frac{\pi}{N}(k-l-\delta^i)} e^{-j\pi(1-\frac{1}{N})(k-l-\delta^i)}, \quad \delta^i = \epsilon^i - \epsilon^j \text{ while } i = j, \delta^i = \epsilon^j \quad (2.8)$$

is the interference contribution of the l -th subcarrier of the i -th user to the k -th

subcarrier of user j , and $N_k = \frac{1}{N} \sum_{n=0}^{N-1} n[n] e^{-\frac{j2\pi}{N}nk}$ is the AWGN noise on the intended subcarrier in frequency domain.

Under the system configuration with the block assignment of symbols, the problem of CFOs in OFDMA system becomes a linear system problem:

$$\mathbf{Z} = \mathbf{I}\mathbf{H}\mathbf{C} + \mathbf{N} \quad (2.9)$$

We assume the block interleave in the sequence of their indices of subscribers. The l -st user transmits symbols with the l -st block, the 2 -nd user transmit symbol with the 2 -nd block, and so on. Each subscriber uses the equal size of subcarriers M , where $M=N/U$. In this way, $\mathbf{Z} = [(\underline{\mathbf{z}}^1)^T, (\underline{\mathbf{z}}^2)^T, \dots, (\underline{\mathbf{z}}^{U-1})^T, (\underline{\mathbf{z}}^U)^T]^T$ is an N by l matrix, and the entry is the block symbols of the IFFT output, whose size is M by l .

$\mathbf{I} = \begin{bmatrix} \underline{\mathbf{I}}^{1,1} & \dots & \underline{\mathbf{I}}^{1,U} \\ \vdots & \ddots & \vdots \\ \underline{\mathbf{I}}^{U,1} & \dots & \underline{\mathbf{I}}^{U,U} \end{bmatrix}$ is the total interference matrix. The submatrix $\underline{\mathbf{I}}^{l,k}$ means the interference block contributed to the l -th block signals by the k -th block signals, and

$\underline{\mathbf{I}}^{l,k} = \begin{bmatrix} I_{(l-1)M+1, (k-1)M+1} & \dots & I_{(l-1)M+1, kM} \\ \vdots & \ddots & \vdots \\ I_{lM, (k-1)M+1} & \dots & I_{lM, kM} \end{bmatrix}$ is composed of the interference distributed

by the subcarrier of its column index to the subcarrier of its row index.

$\mathbf{H} = \begin{bmatrix} \underline{\mathbf{H}}^1 & 0 & \dots & 0 \\ 0 & \ddots & \ddots & \vdots \\ \vdots & \ddots & \ddots & 0 \\ 0 & \dots & 0 & \underline{\mathbf{H}}^U \end{bmatrix}$, where $\underline{\mathbf{H}}^i = \begin{bmatrix} H_{(i-1)M+1}^i & & \\ & \ddots & \\ & & H_{iM}^i \end{bmatrix}$ is a diagonal matrix, and

the entries are channel impulse response values in frequency domain of the i -th subscriber's subcarriers. In other words, the total channel impulse response \mathbf{H} in frequency domain is also a diagonal matrix and is composed of the channel responses

of various subscribers. $\mathbf{C} = \sum_{i=1}^U \mathbf{c}^i$ is the sum of transmitted signals after interleaving.

With the proper arrangement of block subcarriers, different blocks of subcarriers would not be overlapped so that \mathbf{C} becomes:

$$\mathbf{C} = \left[\mathbf{c}_0^1, \dots, \mathbf{c}_{M-1}^1, \mathbf{c}_M^2, \dots, \mathbf{c}_{2M-1}^2, \dots, \mathbf{c}_{(U-1)M}^U, \dots, \mathbf{c}_{UM-1}^U \right]^T = \left[(\mathbf{c}^1)^T, (\mathbf{c}^2)^T, \dots, (\mathbf{c}^U)^T \right]^T \quad (2.10)$$

\mathbf{N} is the AWGN noise vector. Equation $\mathbf{Z} = \mathbf{IHC} + \mathbf{N}$ becomes:

$$\begin{bmatrix} \mathbf{z}^1 \\ \vdots \\ \mathbf{z}^U \end{bmatrix} = \begin{bmatrix} \mathbf{I}^{1,1} & \dots & \mathbf{I}^{1,U} \\ \vdots & \ddots & \vdots \\ \mathbf{I}^{U,1} & \dots & \mathbf{I}^{U,U} \end{bmatrix} \begin{bmatrix} \mathbf{H}^1 & \mathbf{0} \\ \vdots & \ddots \\ \mathbf{0} & \mathbf{H}^U \end{bmatrix} \begin{bmatrix} \mathbf{c}^1 \\ \vdots \\ \mathbf{c}^U \end{bmatrix} + \begin{bmatrix} \mathbf{N}^1 \\ \vdots \\ \mathbf{N}^U \end{bmatrix} \quad (2.11)$$

, and let further focus on the i -th subscriber's block signal:

$$\mathbf{z}^i = \sum_{k=1}^U \mathbf{I}^{i,k} \mathbf{H}^k \mathbf{c}^k + \mathbf{N}^i = \mathbf{I}^{i,i} \mathbf{H}^i \mathbf{c}^i + \sum_{\substack{k=1, \\ k \neq i}}^U \mathbf{I}^{i,k} \mathbf{H}^k \mathbf{c}^k + \mathbf{N}^i \quad (2.12)$$

The first term is the desired block signal with the interference caused by subcarriers inter block itself. The second term is the multiuser interference (MAI). The third term is AWGN noise.

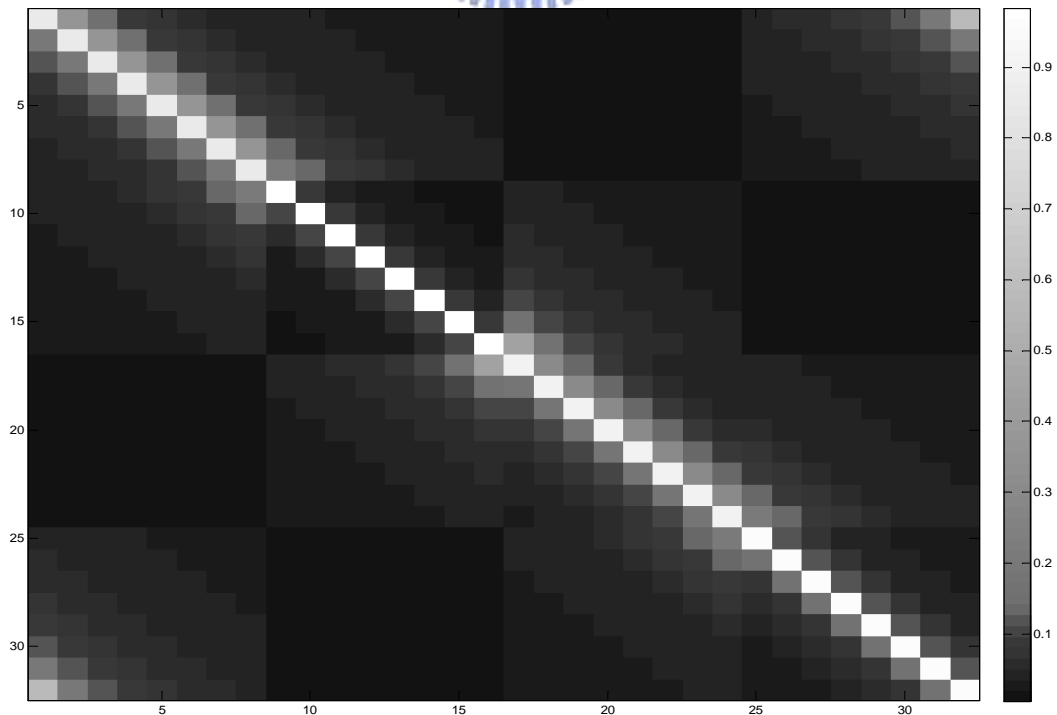


Figure 2.3.3 Image of interference matrix in OFDMA system

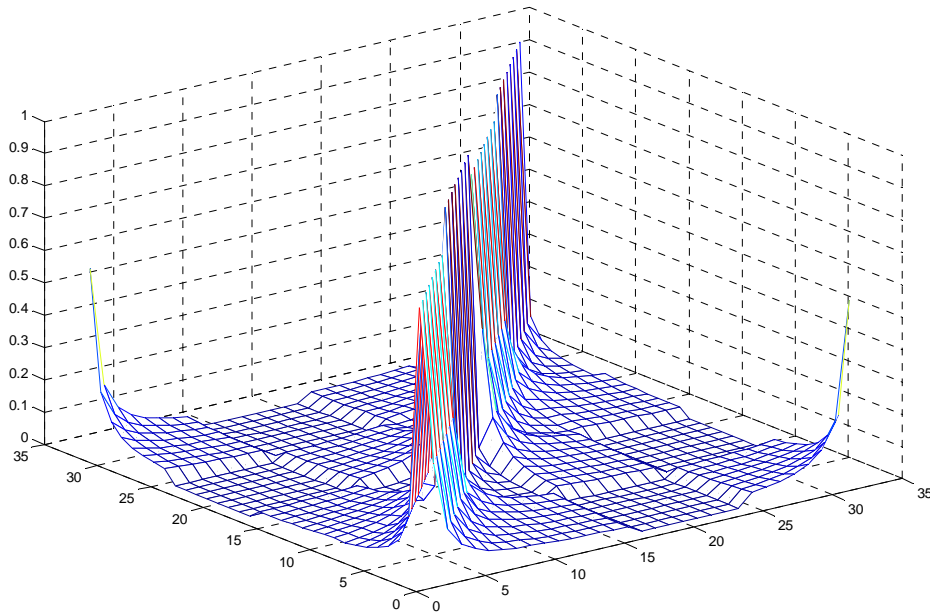


Figure 2.3.4 Mesh of amplitude to interference matrix in OFDMA system

The figures above are the examples illustrating the concept of interference matrix.

The figures are depicted under the conditions:

- ◆ total number of subcarriers: $N=32$
- ◆ the number of subscribers: $U=4$
- ◆ the relative CFOs: $\varepsilon^1 = 0.3$, $\varepsilon^2 = -0.1$, $\varepsilon^3 = 0.25$, $\varepsilon^4 = -0.15$

The first figure is the image of interference matrix \mathbf{H} whose colormap in matlab is “Gray”, and the second figure is the mesh of interference matrix \mathbf{H} . In both two figures, it is apparent to know that the most significant amplitude of interference happens at the diagonal entries and decreases progressively with leaving of diagonal. The major difference between OFDM and OFDMA is that \mathbf{H} of OFDM is a Toeplitz matrix, and \mathbf{H} of OFDMA is composed of submatrices. Each submatrix is dominated by the relative CFO.

2.4. Methods of Reducing Interference due to Carrier Frequency

Offset in OFDMA System

The strategies to CFOs in OFDM in section 2.2 are self-interference cancelling [11] and windowing [11][13]. However, the self-interference cancellation method is less bandwidth efficient than the original OFDM. The windowing approach will reduce the overall SNR comparing with the OFDM system without windowing.

In this section, we introduce some methods of solving the CFOs problem in the OFDMA system: I. Interference Cancellation (IC) based OFDMA receivers II. Least squares (LS) and Minimum mean square error (MMSE) based methods.

A. IC based OFDMA receivers-Successive Interference Cancellation

In the literature [23], Successive Interference Cancellation (SIC) is used to solve the CFO problem in the OFDMA system. The received signals after FFT operation are ranked according to their subcarrier power: The principal of successive IC scheme is base on the strongest signal.

We can pick up and detect the strongest signal. The interference induced by this signal is reconstructed first and then removed recursively from the rest of signals. This procedure continues until all the signals were picked and detected.

In figure 2.4.1, the received signals were ranked by their own power ($\mathbf{Z} \rightarrow \mathbf{Z}'$), and the lower index was the order. z_q^j is represented as the q -th big signal of all, which belongs to the j -th user. The device “Interference cancellation and Signal passing” cancels the interference $\hat{\mathbf{I}}_q^j \hat{H}_q^j \hat{c}_q^j$ of the last detected signal \hat{c}_q^j and then send the next signal z_{q+1}^j for iteration.

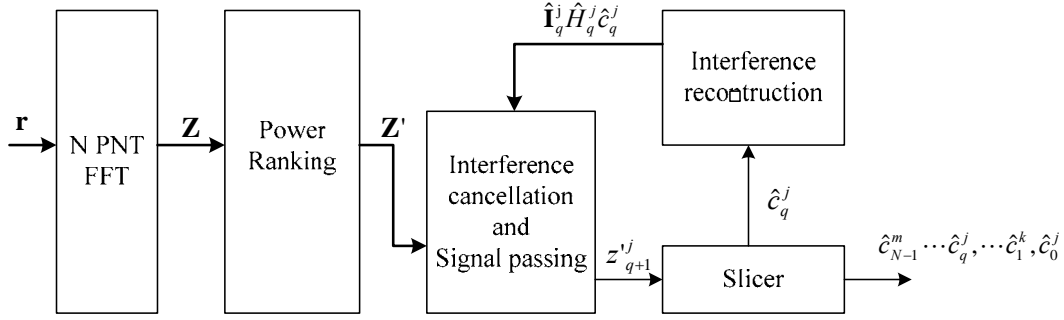


Figure 2.4.1 Block diagram of successive interference cancellation in OFDMA system

Algorithm:

Initialization: ($q=0$)

$$\hat{c}_0^j = \text{slice}(z_0^j) \quad (2.13)$$

Loop: ($q=1, 0, \dots, N-1$)

$$(\mathbf{Z}')^q = (\mathbf{Z}')^{q-1} - \hat{\mathbf{I}}_{q-1}^j \hat{H}_{q-1}^j \hat{c}_{q-1}^j \quad (2.14)$$

$$\hat{c}_q^j = \text{slice}(z_q^j) \quad (2.15)$$

Go back to loop

At the initialization, the algorithm slices the first subcarrier of ranked signal z_0^j , which belongs to the j -th user, and obtain a detected signal \hat{c}_0^j . Then it goes to a loop to reconstruct the interference resulted from the previous detected signal. $\hat{\mathbf{I}}^j$ and \hat{H}^j are the estimates of the interference term and channel response, respectively. The interference term depends on the frequency offset estimates. After the cancellation of the last detected signal (eq. 2.18), the device passes the following ranked signal for detection (eq. 2.19). In this way, it iterates $N-1$ time to obtain the final signal.

The problem of SIC is the principle of ranking signals. The strongest signal is not necessarily the most reliable signal. The signal components might be contributed by the interference from other subcarriers. The interference is enormous when the CFO increases. The performance degradation becomes unacceptable. .

B. Least squares and Minimum mean square error based methods

In literature [21], the LS and MMSE criteria are applied to reconstruct the orthogonal spectral signals based on the estimated CFOs at the uplink receiver.

Algorithm and implementation:

In the LS and MMSE based approaches, the signal of OFDMA uplink at the receiver is modeled as:

$$\mathbf{Z} = \mathbf{I}\mathbf{H}\mathbf{C} + \mathbf{N} = \mathbf{I}\mathbf{S} + \mathbf{N} \quad (2.16)$$

where \mathbf{Z} is the received signal vector N by I , \mathbf{I} is the interference mentioned in section 2.3.3, \mathbf{H} is an N by N matrix channel impulse response of total subcarriers in frequency domain, \mathbf{C} is an N by I vector of the source signal information, \mathbf{N} is an AWGN noise vector, and \mathbf{S} is the combined signal vector of channel impulse response and source signal information.

The first criterion is the minimum sum of noise energy in OFDMA received signal block. This leads to the result of least square (LS) method:

$$\mathbf{S}_{LS}^* = (\mathbf{I}^H \mathbf{I})^{-1} \mathbf{I}^H \mathbf{Z} \quad (2.17)$$

The second criterion is the minimum mean square error. Different from the LS method, the MMSE method assumes that the second order statistics of the signals and the noise are known at the uplink receiver. Assume the noise at each subscriber is AWGN with zero mean and the covariance σ_n^2 and $\mathbf{E}[\mathbf{N}\mathbf{N}^H] = \sigma_n^2 \mathbf{I}_d$, where \mathbf{I}_d is an N by N identity matrix. $\mathbf{E}[*]$ denotes the expectation value. The MMSE solution

is given by:

$$\mathbf{S}_{MMSE}^* = \mathbf{R}\mathbf{I}^H (\mathbf{I}\mathbf{R}\mathbf{I}^H + \sigma_n^2 \mathbf{I}_d)^{-1} \mathbf{Z}, \quad (2.18)$$

where \mathbf{R} is the autocorrelation matrix of the orthogonal spectral signal \mathbf{S} as $\mathbf{R} = \mathbf{E}[\mathbf{S}\mathbf{S}^H]$. If the average power σ_s^2 of the received orthogonal spectral signal at

all subcarriers are the same, it will be $\mathbf{R} = \mathbf{E}[\mathbf{S}\mathbf{S}^H] = \sigma_s^2 \mathbf{I}_d$. The result of the previous

MMSE method becomes:

$$\mathbf{S}_{MMSE}^* = \mathbf{I}^H (\mathbf{I}\mathbf{I}^H + \frac{\sigma_n^2}{\sigma_s^2} \mathbf{I}_d)^{-1} \mathbf{Z} \quad (2.19)$$

However, the computation complexity of this algorithm is high. Furthermore, in contrast with the block based OFDMA system [22], the complexity of MMSE receiver in interleaved subcarrier systems is fairly high [21].



3. Block Based Carriers Frequency Offset Cancellation Schemes

In the textbook [24], "Multiuser Detection," of Verdu, the author mentioned the Multistage Detection approach. Because the cancellation order of multi-user interference greatly affects the performance of the successive cancellation for a particular user, Verdu explored a symmetrical version of successive cancellation, which mitigates the shortcomings of conventional successive cancellation.

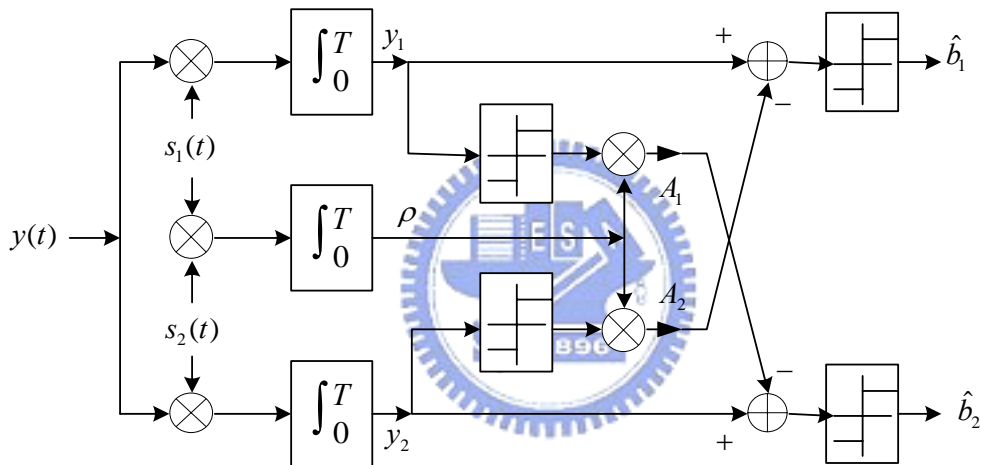


Figure 3.0.1 Concept of conventional multistage detection (two stages type)

Figure 3.0.1 illustrates the concept of conventional two stages multistage detection for two users. In the first stage, the conventional bank of single user matched filter is used, whereas in the second stage successive cancellation is used for both users. This approach can even be extended to iteratively processing by cleaning up the original matched filter outputs. Moreover, the multistage approach can use the tentative decisions rather than those provided by bank of single-user matched filters.

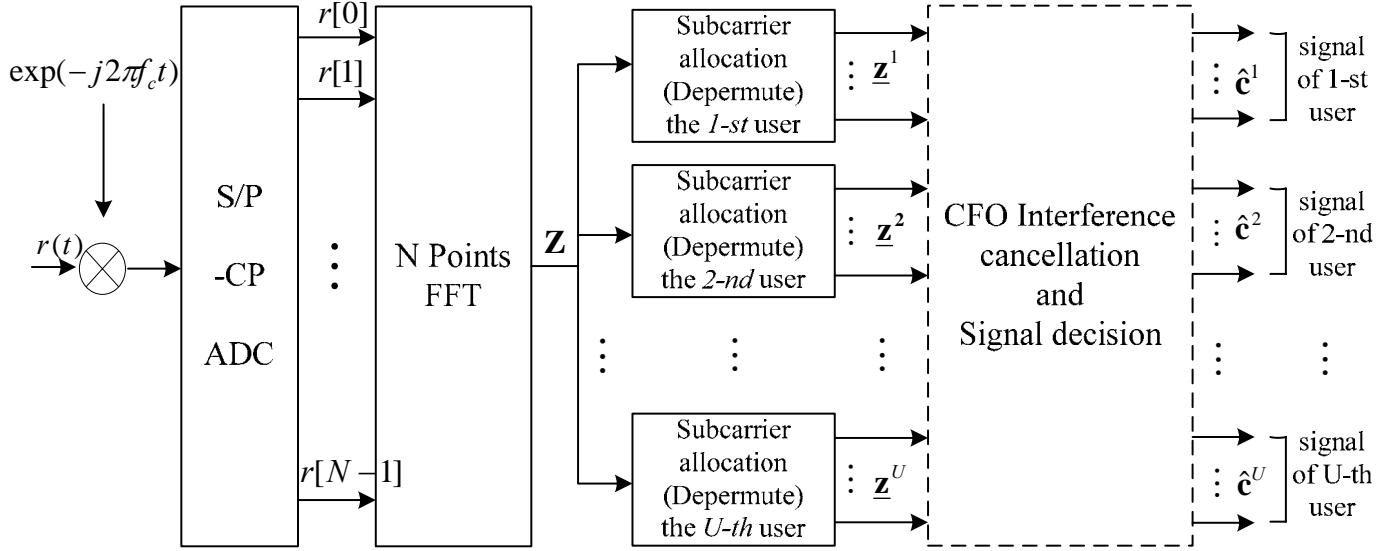


Figure 3.0.2 Receiver at the base station of OFDMA uplink

Figure 3.0.2 shows the receiver architecture mentioned in section 1.4.4. The dashed line block is the CFO interference cancellation we propose. The details are as follows.

From the derivation in section 2.3, the desired block signals of *the i-th* user after demodulation can be expressed as:

$$\underline{\mathbf{z}}^i = \sum_{k=1}^U \underline{\mathbf{I}}^{i,k} \underline{\mathbf{H}}^k \underline{\mathbf{c}}^k + \underline{\mathbf{N}}^i = \underline{\mathbf{I}}^{i,i} \underline{\mathbf{H}}^i \underline{\mathbf{c}}^i + \sum_{\substack{k=1, \\ k \neq i}}^U \underline{\mathbf{I}}^{i,k} \underline{\mathbf{H}}^k \underline{\mathbf{c}}^k + \underline{\mathbf{N}}^i = (\text{signals+ICI}) + \text{MUI} + \text{Noise} \quad (3.1)$$

The first term is the desire block with ICI, the second is MAI, and the third is AWGN. Because of the Toeplitz property of the ICI submatrix (described in section 2.3), the computation of its inversion can be implemented by the Trench algorithm [25], which is more efficient and easier to realize in digital circuit than the algorithm of regular matrix inversion. We can suppress and eliminate the interference resulting from ICI by $(\underline{\mathbf{I}}^{i,i})^{-1}$. In addition, if the CSI is well estimated, the channel impulse

response in frequency domain $\underline{\mathbf{H}}^i$ can be constructed. In this way, eliminating ICI and compensating the channel effect are possible; Multiplying the inversion of the combination matrix, $\underline{\mathbf{I}}^{i,i} \underline{\mathbf{H}}^i$, we can obtain the signals:

$$\begin{aligned} (\underline{\mathbf{I}}^{i,i} \underline{\mathbf{H}}^i)^{-1} \underline{\mathbf{z}}^i &= (\underline{\mathbf{I}}^{i,i} \underline{\mathbf{H}}^i)^{-1} \underline{\mathbf{I}}^{i,i} \underline{\mathbf{H}}^i \underline{\mathbf{c}}^i + (\underline{\mathbf{I}}^{i,i} \underline{\mathbf{H}}^i)^{-1} \sum_{\substack{k=1, \\ k \neq i}}^U \underline{\mathbf{I}}^{i,k} \underline{\mathbf{H}}^k \underline{\mathbf{c}}^k + (\underline{\mathbf{I}}^{i,i} \underline{\mathbf{H}}^i)^{-1} \underline{\mathbf{N}}^i \\ &= \underline{\mathbf{c}}^i + (\underline{\mathbf{I}}^{i,i} \underline{\mathbf{H}}^i)^{-1} \sum_{\substack{k=1, \\ k \neq i}}^U \underline{\mathbf{I}}^{i,k} \underline{\mathbf{H}}^k \underline{\mathbf{c}}^k + (\underline{\mathbf{I}}^{i,i} \underline{\mathbf{H}}^i)^{-1} \underline{\mathbf{N}}^i \end{aligned} \quad (3.2)$$

The desire block signals in the first term are purified and more reliable than other terms. The interference cancellation procedure can be represented as the bank of single-user matched filters in the multistage detection. With the good symbol detector, the block signals of the i -th are then detected:

$$\hat{\underline{\mathbf{c}}}^i = \text{detector}((\underline{\mathbf{I}}^{i,i} \underline{\mathbf{H}}^i)^{-1} \underline{\mathbf{z}}^i) \quad (3.3)$$

Combine the IC based schemes and the multistage detection. We propose two CFO interference cancellation approaches which can benefit from frequency diversity and have low computation in the following sections. The methods are:

1. Block Parallel Interference Cancellation (BPIC)
2. Block Successive Interference Cancellation (BSIC)

3.1. Block Parallel Interference Cancellation

The spirit of the BPIC scheme originates from the multistage detection. The symmetrical and parallel structures are the features of the system. Thus it is fair to every user [24]. Figure 3.1.1 shows the block diagram of BPIC. The system can be iteratively processed, and the number of stage is equal to the number of iteration

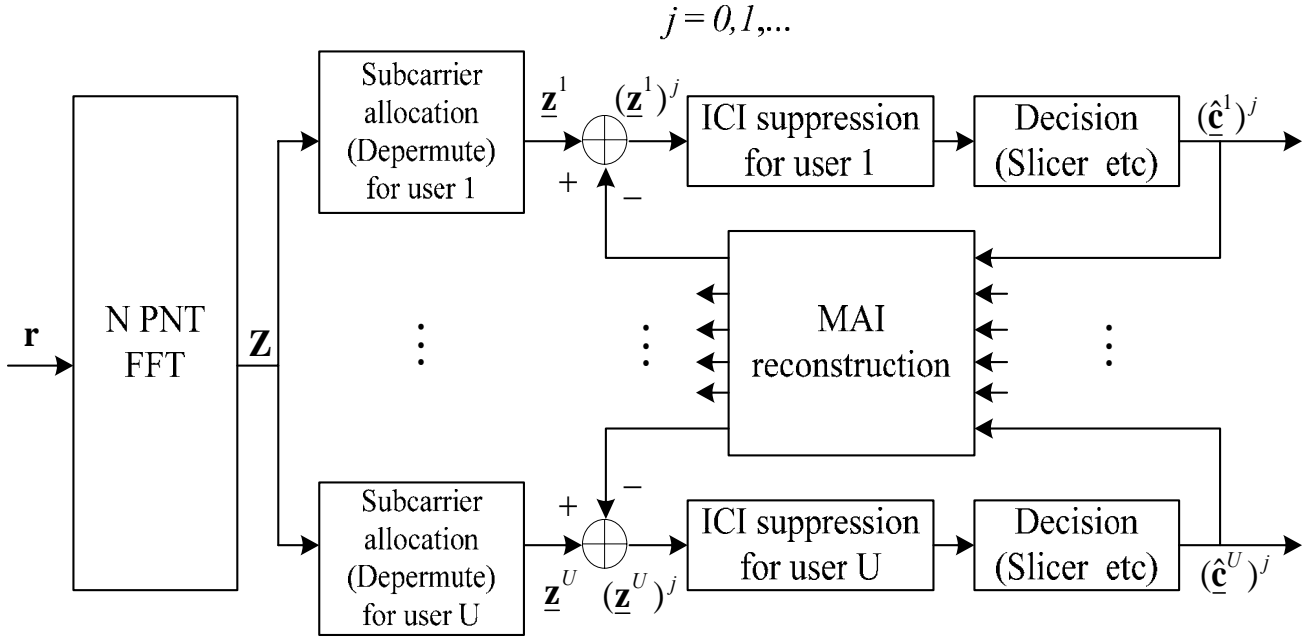


Figure 3.1.1 Block diagram of block parallel interference cancellation



Algorithm:

Initialization: $j = 0$

SET

$$\begin{aligned}
 (\hat{\mathbf{c}}^i)^j &= \text{detector}((\mathbf{I}^{i,i} \mathbf{H}^i)^{-1} \mathbf{z}^i) \\
 &= \text{detector}(\hat{\mathbf{c}}^i + (\mathbf{I}^{i,i} \mathbf{H}^i)^{-1} \sum_{\substack{k=1, \\ k \neq i}}^U \mathbf{I}^{i,k} \mathbf{H}^k \hat{\mathbf{c}}^k + (\mathbf{I}^{i,i} \mathbf{H}^i)^{-1} \mathbf{N}^i), \quad (3.4)
 \end{aligned}$$

for $i = 0, 1, \dots, U$, where $\mathbf{z}^i = (\mathbf{T}^i)^T \mathbf{Z}$

Loop: $j = j + 1$

SET

$$(\mathbf{z}^i)^j = \mathbf{z}^i - \sum_{\substack{k=1, \\ k \neq i}}^U \mathbf{I}^{i,k} \mathbf{H}^k (\hat{\mathbf{c}}^k)^{j-1}, \text{ for } i = 0, 1, \dots, U$$

(3.5)

$$(\hat{\mathbf{c}}^i)^j = \text{detector}((\mathbf{I}^{i,i} \mathbf{H}^i)^{-1} (\mathbf{z}^i)^j), \text{ for } i = 0, 1, \dots, U \quad (3.6)$$

Go back to loop

As shown in figure 3.1.1, after de-permutation of demodulated signals, the signals $\underline{\mathbf{z}}^i, i=1, \dots, U$ are sent to the paths of their subscriber. In the first stage of BPIC, similar to the multistage detection, the signal was multiplied by the inversion of $\underline{\mathbf{I}}^{i,i} \underline{\mathbf{H}}^i$, where the index i varies with the subscriber. This operation matches the desire block signals. In other words, this will suppress the ICI in the block itself and compensate the channel effect. Meanwhile, the desired block signals are purified and become more reliable than before. The detected signal $(\hat{\underline{\mathbf{c}}})^j, i=1, \dots, U$ in eq.3.4 will be used for MAI reconstruction. The device, “MAI reconstruction,” collects all the detected signals and reconstructs MAI of each path for MAI elimination in the next stage.

In the second stage, we first use the results of the last iteration to eliminate the MAI from the signals after de-permutation in eq.3.5. Then, the signals $(\underline{\mathbf{z}}^i)^j, i=1, \dots, U$ with less MAI will be ready for the first stage operation (eq.3.6) of the next iteration.

It is known that the parallel interference cancellation structure processes the signals in parallel and has high computation requirement. To acquire higher performance without increasing computation complexity, another scheme is proposed in the next section.

3.2. Block Successive Interference Cancellation

In section 2.3.3, we know that the total interference matrix is composed of submatrices. The major interference happens in the diagonal submatrix, and the diagonal submatrix is subject to the CFO. In this reason, the CFOs can be taken as the

principle about the reliability.

In the BSIC schemes, the SIC structure is employed in the first iteration. Instead of ranking the order by power, we rank the block signal by the CFOs. The smaller CFO it is, the more reliable the signal is.

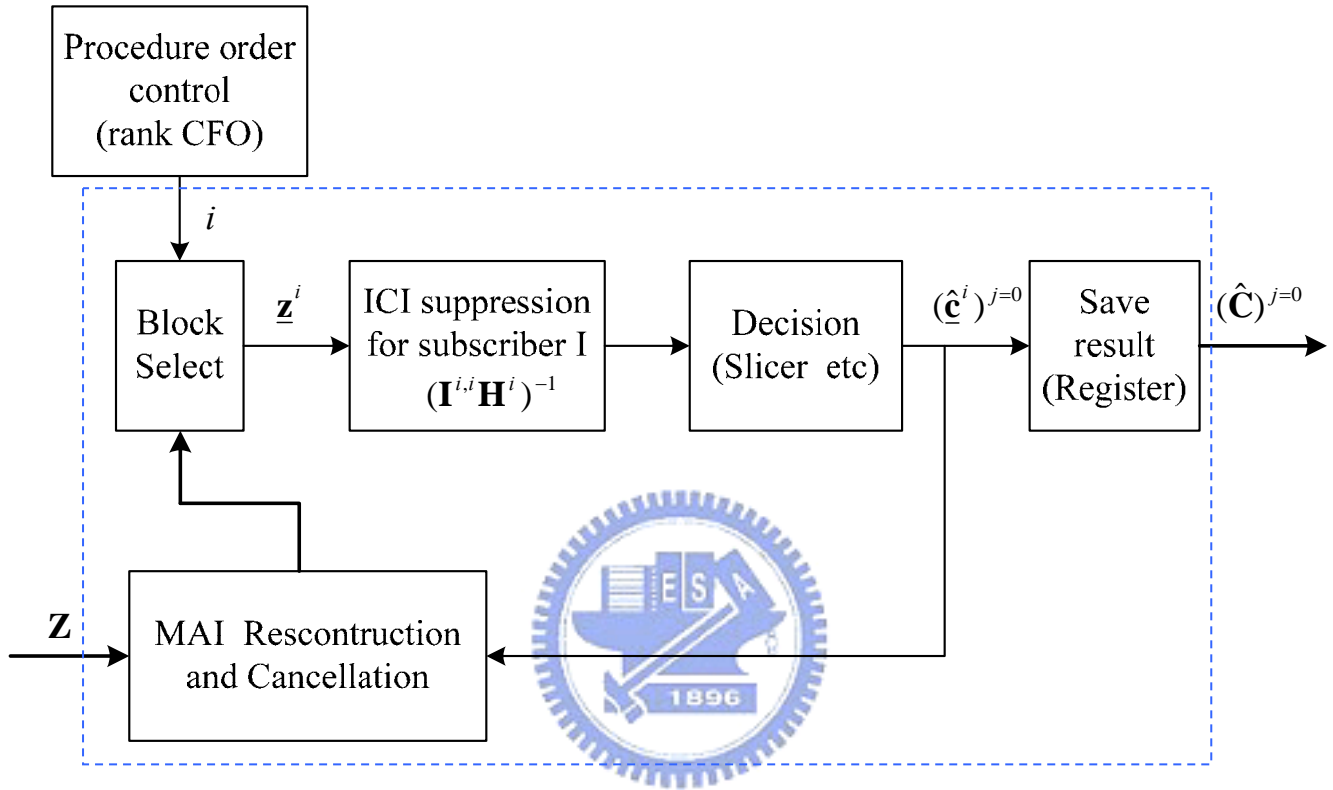


Figure 3.2.1 Block diagram of BSIC the first iteration

Figure 3.2.1 illustrates the block diagram of the first-iteration BSIC. Apparently, this is a SIC structure. The procedure order control ranks the estimated CFOs and sends the chosen index to the “Block Select” device. The chosen block \underline{z}^i is then ICI-suppressed before the decision. The detected block signal $(\hat{\underline{c}}^i)^{j=0}$ is then kept in the register for the next iteration of processing. On the other side, the decided signal is fed back to “MAI reconstruction and Cancellation” device. The device reconstructs the interference components to the other users and cancels from the signals. In this way, the cancelled signals become more reliable than the signals without any

cancellation, and that will benefit the following iteration.

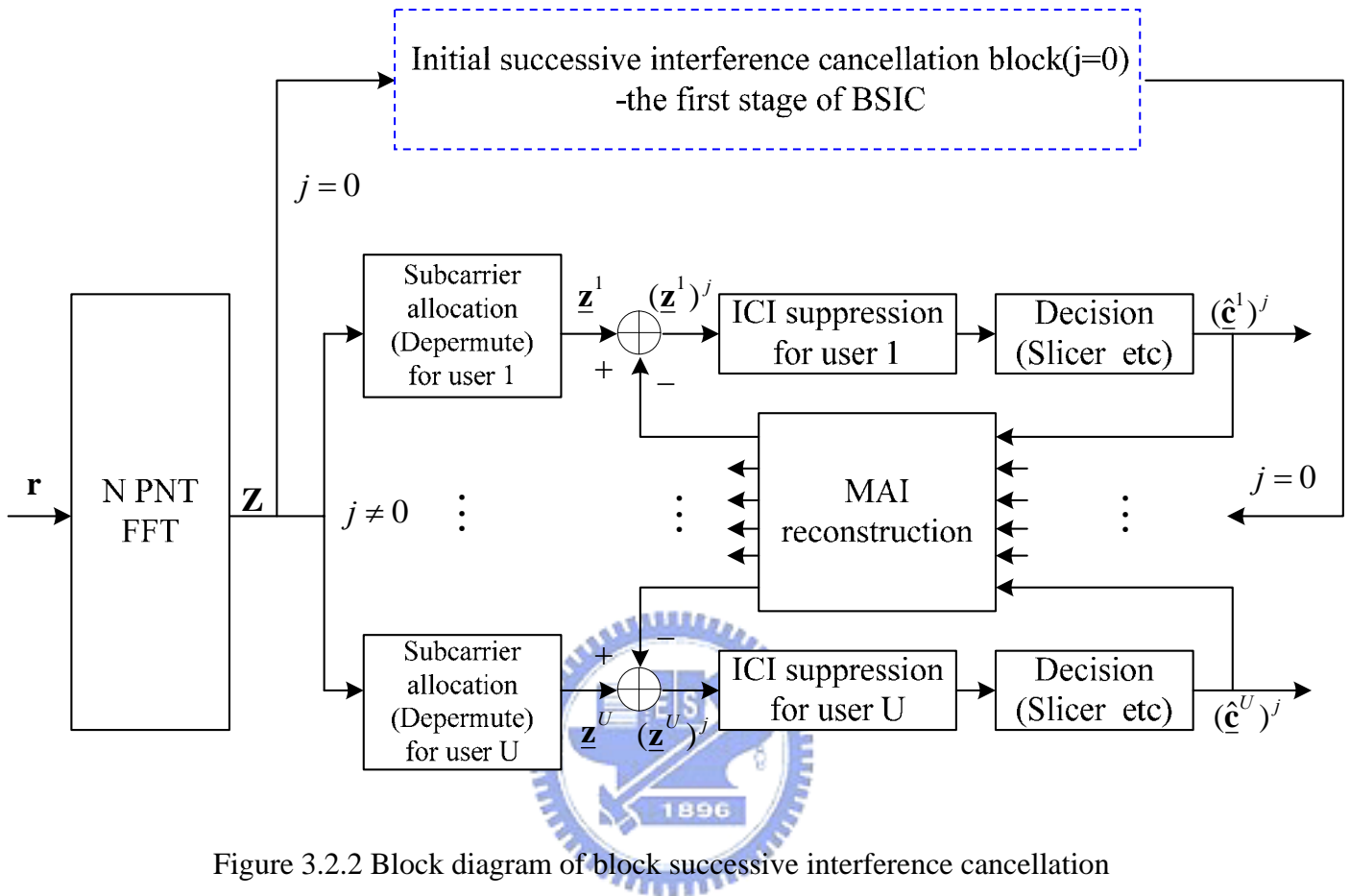


Figure 3.2.2 Block diagram of block successive interference cancellation

The decided signal $(\hat{\mathbf{C}})^{j=0}$ in first stage is used as the input of the next iteration of processing. Using the results of BSIC in first stage, the MAI reconstruction rebuilds the MAI of each block for the next iteration. Figure 3.3.2 shows the block diagram of the BSIC scheme. The algorithm of BSIC is as below:

Algorithm:

Initialization: $j = 0$

Rank the estimated CFOs of each subscriber

$d = 0$

Loop: $d = d + 1$

Select the un-chosen block of smallest CFO: i

$$\begin{aligned} (\hat{\mathbf{c}}^i)^j &= \text{detector}((\mathbf{I}^{i,i} \mathbf{H}^i)^{-1} \mathbf{z}^i) \\ &= \text{detector}(\mathbf{c}^i + (\mathbf{I}^{i,i} \mathbf{H}^i)^{-1} \sum_{\substack{k=1, \\ k \neq i}}^U \mathbf{I}^{i,k} \mathbf{H}^k \mathbf{c}^k + (\mathbf{I}^{i,i} \mathbf{H}^i)^{-1} \mathbf{N}^i), \end{aligned} \quad (3.7)$$

where $\mathbf{z}^i = (\mathbf{T}^i)^T \mathbf{Z}$

$$\mathbf{z}^l = \mathbf{z}^l - \mathbf{I}^{l,i} \mathbf{H}^i (\hat{\mathbf{c}}^i)^{j=0}, \text{ for } l = 1, 2, \dots, U \text{ and } l \neq i \quad (3.8)$$

Go back to Loop until $d=U-1$.

Reload $\mathbf{z}^l, l = 1, 2, \dots, U$ from \mathbf{Z}' .

Loop: $j = j + 1$

SET

$$(\mathbf{z}^i)^j = \mathbf{z}^i - \sum_{\substack{k=1, \\ k \neq i}}^U \mathbf{I}^{i,k} \mathbf{H}^k (\hat{\mathbf{c}}^k)^{j-1}, \text{ for } i = 0, 1, \dots, U \quad (3.9)$$

$$(\hat{\mathbf{c}}^i)^j = \text{detector}((\mathbf{I}^{i,i} \mathbf{H}^i)^{-1} (\mathbf{z}^i)^j), \text{ for } i = 0, 1, \dots, U \quad (3.10)$$

Go back to loop

The BSIC scheme takes longer delay than the BPIC when there are a large number of users. However, the weak users' signal can be purified with MAI cancellation in the first iteration of BSIC. Thus, the BSIC outperforms the BPIC. Moreover, the BPIC scheme directly uses the parallel structure to eliminate all the ICIs simultaneously. The BSIC scheme employs the successive cancellation structure to eliminate the each individual user's MUI in the undecided block signal.

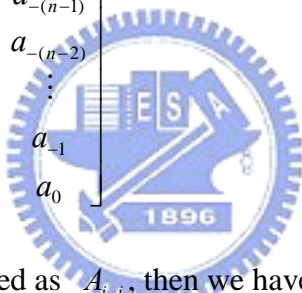
Both the BPIC and the BSIC algorithms require the matrix inversion computation. Normally, it takes the $O(n^3)$ operations to complete the matrix inversion of an arbitrary $n \times n$ system by using the Gaussain factorization (One

operation consists of one complex multiplication and roughly one complex addition). Fortunately, the interference submatrix is a Toeplitz matrix, which has the fast computation algorithm to complete the inversion. In the next section, the inversion computation of a Toeplitz matrix will be described.

3.3. Computation to Inversion of Toeplitz Matrix

3.3.1. Toeplitz matrix

In the theory of linear algebra, a Toeplitz matrix, named after Otto Toeplitz, is a matrix in which each descending diagonal from left to right is constant. For instance, the $n \times n$ Toeplitz matrix A is of the form

$$\mathbf{A} = \begin{bmatrix} a_0 & a_{-1} & \cdots & a_{-(n-2)} & a_{-(n-1)} \\ a_1 & a_0 & \ddots & & a_{-(n-2)} \\ \vdots & \ddots & \ddots & \ddots & \vdots \\ a_{n-2} & & \ddots & a_0 & a_{-1} \\ a_{n-1} & a_{n-2} & \cdots & a_1 & a_0 \end{bmatrix} \quad (3.11)$$


If the i, j element of A is denoted as $A_{i,j}$, then we have

$$A_{i,j} = a_{i-j} \quad (3.12)$$

The study of Toeplitz linear equations arises in many applications, ie, analysis of stationary time series, digital signal processing, image filtering, estimation theory, etc. In 1947 Levinson gave an efficient recursive algorithm for solving the set of Hermitian-Toeplitz equations. Trench extended Levinson's result to obtain an efficient way of inverting a Toeplitz matrix. Based on Trench's work, Zohar proposed an algorithm that requires less computation than the previous algorithms. Latter, it came out variety of fast algorithms for the Toeplitz matrix calculation. However, most of them are suitable for Hermitian-Toeplitz case. To meet our needs, we employ the Trench algorithm [25] improved by Zohar.

3.3.2. Trench algorithm

Trench Algorithm was proposed in 1964 by W.F Trench. The method is powerful and elegant. The original Trench algorithm is aimed to solve the Hermitian matrix problems. Zohar modified Trench algorithm so that the calculation is general for all non-Hermitian cases.

Although the inversion algorithm can be used for the non-Hermitian case, not all the Toeplitz matrices are applicable. The requirement of this inversion algorithm is that the matrix must be “strongly nonsingular.” An arbitrary matrix is said to be strongly non-singular when, the matrix is nonsingular and all the principal submatrices must be nonsingular as well. In our CFO cancellation application, the interference submatrices in block based OFDMA system are strongly nonsingular so the fast matrix inversion algorithm can be applied.

Given a Toeplitz matrix L_m , where $m = n + 1$, we consider the i -th order upper-left submatrix L_i . Let us denote the inverse of L_i as B_i , $B_i = L_i^{-1}$. The superscript e on a column vector represents a vector augmented by extra entries. The symbol “ \sim ” denotes transposition. “ $*$ ” is the complex conjugate. The symbol “ \wedge ” on a column vector represents reverse ordering of the entries

Problem formulation:

$$B_{i+1} = \lambda_i^{-1} \begin{bmatrix} 1 & \tilde{e}_i \\ g_i & M_i \end{bmatrix}, \quad L_{n+1} = \begin{bmatrix} 1 & \tilde{a}_n \\ r_n & L_n \end{bmatrix} \quad (3.13)$$

$$\tilde{a}_n = [\rho_{-1} \ \rho_{-2} \ \cdots \ \rho_{-i}] \ (1 \leq i \leq n), \quad \tilde{r}_n = [\rho_1 \ \rho_2 \ \cdots \ \rho_i] \ (1 \leq i \leq n), \quad (3.14)$$

Initial value for recursion:

$$e_1 = -\rho_{-1}, \ g_1 = -\rho_1, \ \lambda_1 = 1 - \rho_{-1}\rho_1 \quad (3.15)$$

Recursion of λ , g , e ($1 \leq i < n$):

$$\eta_i = -(\rho_{-(i+1)} + \tilde{e}_i \hat{a}_i) / \lambda_i \quad (3.16)$$

$$r_i = -(\rho_{i+1} + \tilde{r}_i \hat{g}_i) / \lambda_i \quad (3.17)$$

$$e_{i+1} = \begin{bmatrix} e_i + \eta_i \hat{g}_i \\ \eta_i \end{bmatrix}, \quad \hat{g}_{i+1} = \begin{bmatrix} r_i \\ \hat{g}_i + r_i e_i \end{bmatrix} \quad (3.18)$$

$$\lambda_{i+1} = \lambda_i (1 - \eta_i r_i) \quad (3.19)$$

Evaluation of $B_{n+1} = B_m$:

$$(B_{n+1})_{11} = \frac{1}{\lambda_n} \quad (3.20)$$

$$(B_{n+1})_{1,j+1} = \frac{(e_n)_{j1}}{\lambda_n}, \quad 1 \leq j \leq n \quad (3.21)$$

$$(B_{n+1})_{j+1,1} = \frac{(g_n)_{i1}}{\lambda_n}, \quad 1 \leq i \leq n \quad (3.22)$$

$$(B_{n+1})_{i+1,j+1} = (B_{n+1})_{ij} + \frac{1}{\lambda_n} (g_n \tilde{e}_n - \hat{e}_n \tilde{g}_n)_{ij}, \quad 1 \leq i, j \leq n \quad (3.23)$$

$$(B_{n+1})_{ij} = (B_{n+1})_{n+2-j, n+2-i} \quad (\text{persymmetry}) \quad (3.24)$$

The computation of λ, g, e requires $O(2n^2 - 2n)$ computation. It takes about $O(3n^2)$ computation to obtain the inversion of a non-Hermitian Toeplitz matrix..

4. Computer Simulations and Observations

In order to evaluate the effectiveness of the proposed cancellation schemes, we conduct computer simulations. For the comparison purpose, we also simulate the system proposed in [23] and the system with the simple direct slicer which has no signal compensation..

The fundamental simulation parameters are shown as below:

- ◆ Carrier frequency centered around 2.4GHz
- ◆ Bandwidth of 20MHz
- ◆ Rayleigh fading channel model: # of tapes=4, mean = 0, and variance=1
- ◆ QPSK modulation
- ◆ Size of FFT and IFFT (N): 64
- ◆ Number of subscribers (U): 4 and 8

In the simulation, we perform the matrix inversion based on both the ideal inversion and the Trench algorithm with various CFOs and SNRs so that we can observe the performance loss caused by the Trench algorithm.

4.1. Simulation based Ideal Inversion

We perform the simulation base on proposed BPCI and BSIC schemes in chapter 3. The ideal matrix inversion is applied. In the first experiment, we fix the SNR and increase each user's CFO.

4.1.1. Various CFO sets, Fixed SNR

We assume that all the channel state information (CSI) is perfectly known. The CFOs set we have for the simulation have the fixed frequency difference between every other successive subscribers' CFOs. The Signal to Noise Ration (SNR) is fixed.

When the CFO increases, the interference of ICI is raised,

To observe the performance of receiver, we calculate the SER (Symbol Error Rate) of the different algorithms with various CFOs sets.

A. Number of subscribers: 4

Table of CFOs sets:

Sets' index	1	2	3	4	5	6	7	8
CFO(ppm)	30	40	50	60	70	80	90	100
of each subscribers	40	50	60	70	80	90	100	110
	50	60	70	80	90	100	110	120
	60	70	80	90	100	110	120	130

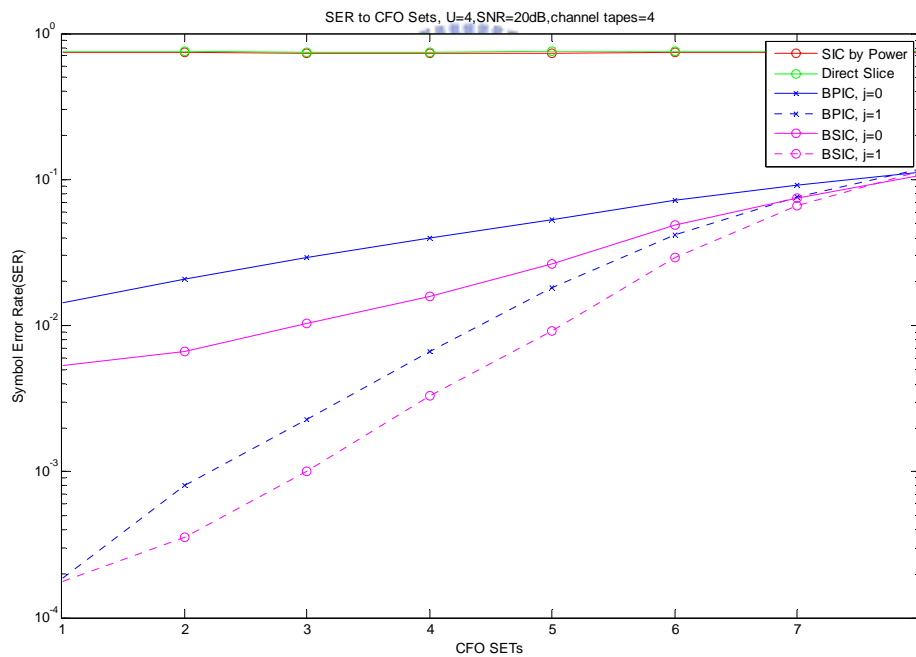


Figure 4.1.1.1 Symbol Error Rate to varying CFO sets, U=4, Rayleigh fading channel tapes=4

In figure 4.1.1.1, the solid lines mean the results of the first stage (iteration), and the dotted lines are the results of the second stage (iteration).

B. Number of subscribers: 8

Table of CFOs sets:

index	CFO (ppm) of each subscribers							
1	20	25	30	35	40	45	50	55
2	30	35	40	45	50	55	60	65
3	40	45	50	55	60	65	70	75
4	50	55	60	65	70	75	80	85
5	60	65	70	75	80	85	90	95
6	70	75	80	85	90	95	100	105

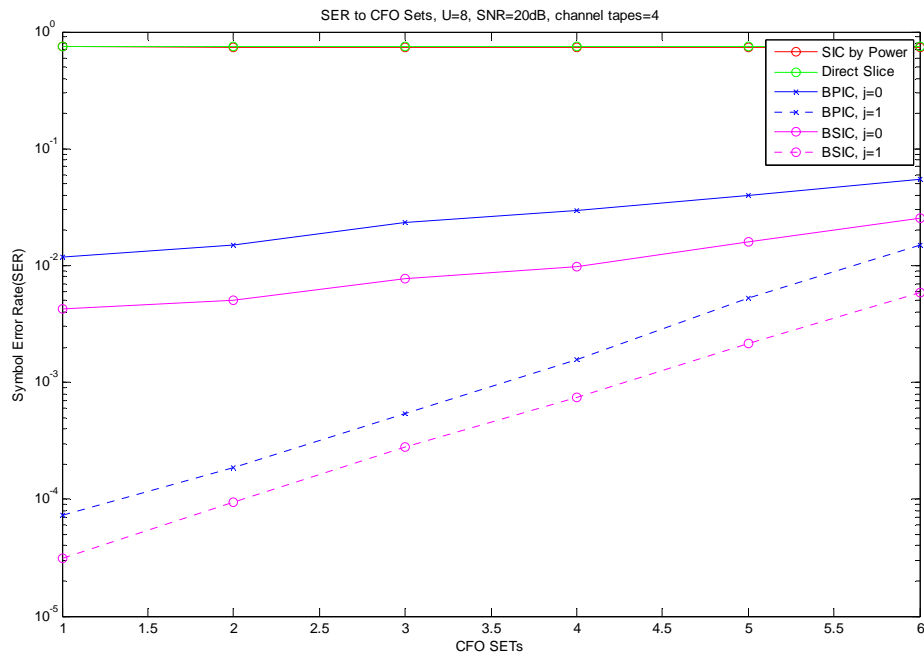


Figure 4.1.1.1 Symbol Error Rate to varying CFO sets, $U=U$, Rayleigh fading channel tapes=4

From the simulation results, both the BPIC and the BSIC schemes work much better than the SIC and the direct slicing schemes. The SIC scheme works well only when the CFO is under 20 ppm and there is no channel effect involved.

The result of the second iteration is better than that of the first iteration. The

elimination of the MUI, which is based on the detected symbols in the previous iteration, does improve the performance in the BSIC scheme. However, in the first iteration the BPIC suppresses the ICI in parallel without MAI elimination. Therefore, the BSIC scheme works better than the BPIC scheme.

When the CFO is large, the correct symbol detection becomes difficult in the first iteration. In this case, increasing the number of iterations does not improve the performance. The SERs of the BSIC ($j=0, j=1$) and the BPIC ($j=1$) are kept under 10^{-2} when the CFOs are greater than 90 ppm.



4.1.2 Various SNR, Fixed CFO Set

In this section, we will observe the SER of the different algorithms with various SNRs and the fixed CFOs set.

In the interference matrix, the amplitude of the submatrices except for the diagonal parts is determined by the difference of CFOs. The energy of the off-diagonal elements reflects the influence of MUI. The most significant MUI is usually caused by the adjacent user. Therefore, we will attempt to observe the effect of the CFO difference of adjacent users in the simulation.

A. Number of subscriber:4

Subscriber's CFO: CFO=[60 20 70 10]

The CFO difference of adjacent users: delta CFO=[40 -50 60 -50]

These values are much larger than the differences in section 4.1.1.

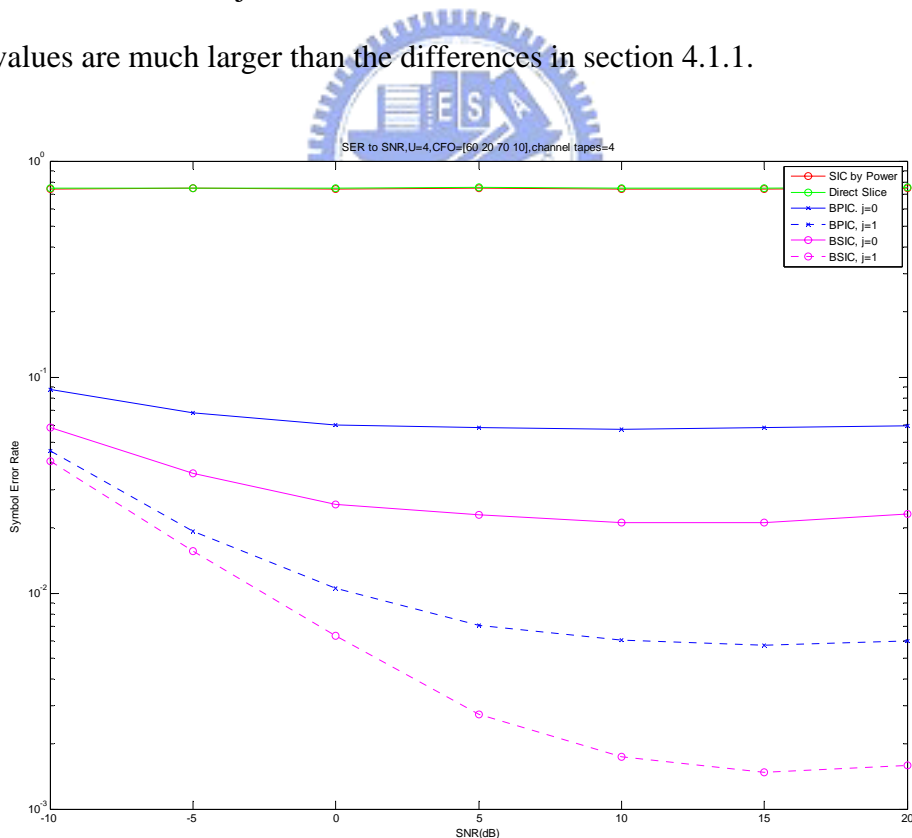


Figure 4.1.2.1 Symbol Error Rate to SNR(dB), U=4, CFO=[60 20 70 10], Rayleigh fading channel tapes=4

B. Number of subscriber:8

Subscriber's CFO: CFO=[40 20 70 10 65 25 75 15]

The difference of the adjacent users: delta CFO=[20 -50 60 -55 40 -50 60 -25].

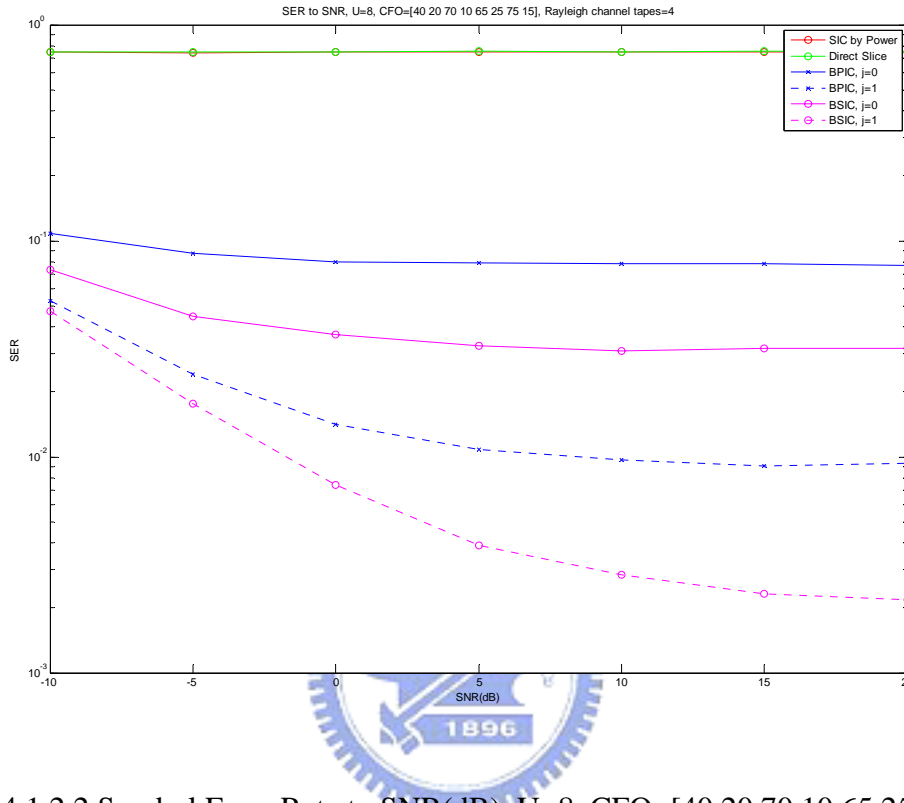


Figure 4.1.2.2 Symbol Error Rate to SNR(dB), U=8, CFO=[40 20 70 10 65 25 75 15], Rayleigh fading channel tapes=4

In figures 4.1.2.2, when the SNR is low, both the BPIC and the BSIC schemes do not have good performance. When the SNR increases, the influence by the noise is reduced and the SER decreases. The SERs finally reach an error floor when the SNR increases.

In contrast to the SIC and the direct slice scheme, the BPIC and the BSIC schemes perform well especially in the second stage (iteration).

The BSIC scheme provides good performance no matter the single stage of processing or the two stage of processing is applied.

4.2. Inversion with Trench Algorithm

In this section, we will see the performance difference when we apply the Trench algorithm to conduct the Toeplitz matrix inversion. We assume that the CSI is known and the simulation parameters are the same as those in the previous sections.

First of all, we show the performance of the Trench algorithm in comparison to the ideal inversion.

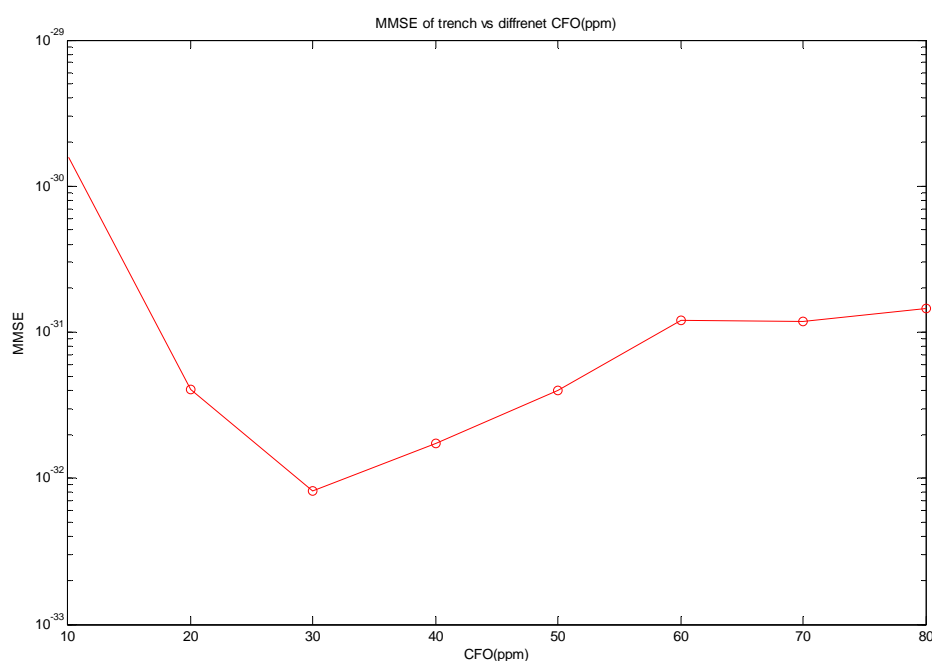


Figure 4.2.0 MMSE to different CFO, Trench Algorithm block size 8 by 8

The figure is the minimum mean square errors (MMSE) of different CFO.

$$MMSE = \text{sum}((\mathbf{B} * \mathbf{L} - \mathbf{I}_d)^2) / m \quad (4.1)$$

where \mathbf{B} is the result of Trench Inversion, \mathbf{L} is the submatrix, and \mathbf{I}_d is an identity matrix. All of them are size m by m . $m=8$ is the size of block subcarrier.

The inverse matrix resulted from the Trench algorithm is very close to the ideal inverse matrix.

We perform the same simulation as the previous section except that the matrix inversion is completed by using the Trench algorithm.

4.2.1. Various CFO Sets, Fixed SNR

The identical experiment in 4.1.1 will be performed again with the Trench algorithm.

A. Number of subscriber:4

Table of CFOs sets:

Sets' index	1	2	3	4	5	6	7	8
CFO(ppm)	30	40	50	60	70	80	90	100
of each	40	50	60	70	80	90	100	110
subscribers	50	60	70	80	90	100	110	120
	60	70	80	90	100	110	120	130

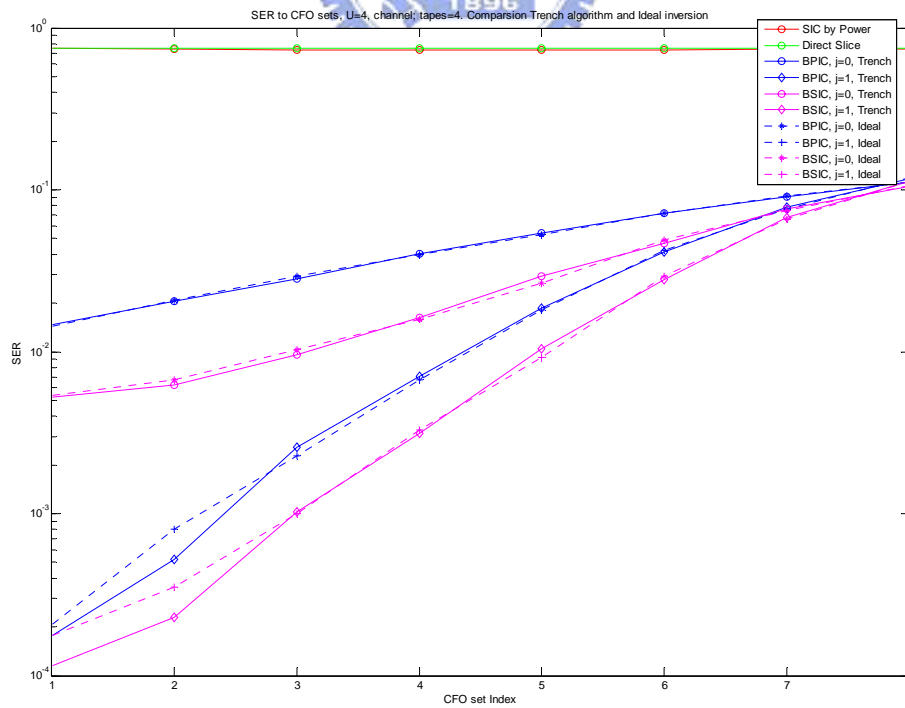


Figure 4.2.1.1 Comparison Trench algorithm and ideal inversion, Symbol Error Rate to varying CFO sets, $U=4$, varying CFO sets, Rayleigh fading channel tapes=4

The comparison between the Trench algorithm and the Ideal inversion can be observed in figure 4.2.1.1. The dotted lines represent the SERs obtained by using the ideal inversion computation result. The solid lines represent the SERs obtained by using the Trench algorithm.

A. Number of subscriber: 8

Table of CFOs sets:

index	CFO (ppm) of each subscribers								
1	20	25	30	35	40	45	50	55	
2	30	35	40	45	50	55	60	65	
3	40	45	50	55	60	65	70	75	
4	50	55	60	65	70	75	80	85	
5	60	65	70	75	80	85	90	95	
6	70	75	80	85	90	95	100	105	

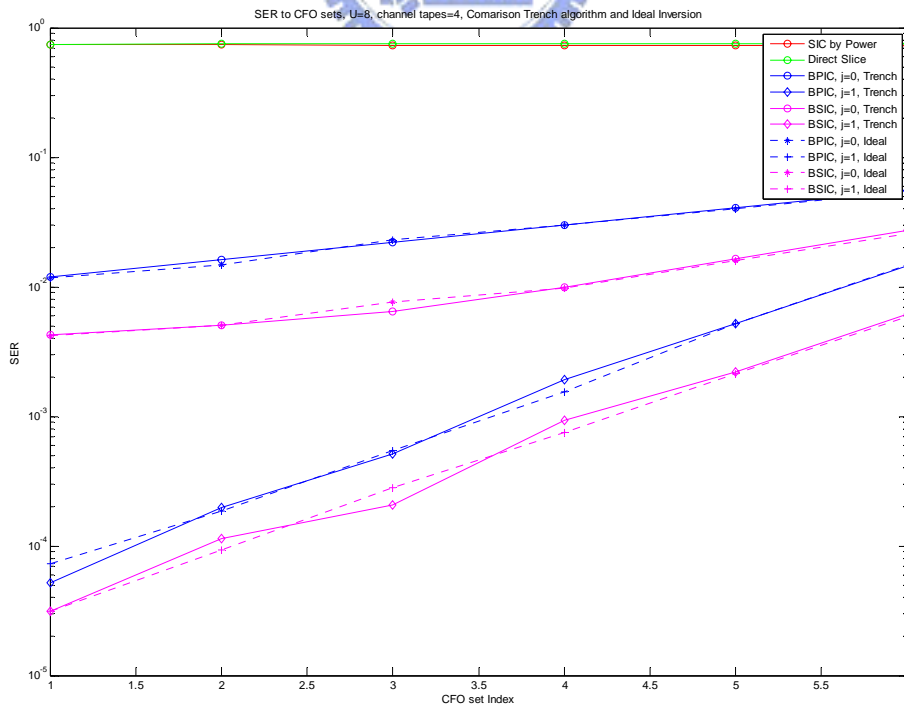


Figure 4.2.1.2 Comparison Trench algorithm and ideal inversion, Symbol Error Rate to varying CFO sets, U=8, varying CFO sets, Rayleigh fading channel tapes=4

In the figures 4.2.1.1 and 4.2.1.2, there is only a slight difference in the performance between the ideal inversion and the Trench algorithm. The Trench algorithm performs well no matter what block sizes or CFOs are applied. The only limitation is that the matrix must be a strongly nonsingular Toeplitz matrix.

4.2.2. Various SNR, Fixed CFO Sets

We repeat the experiments in section 4.1.2 to simulate the propose schemes with the Trench algorithm.

A. Number of subscriber:4

Subscriber's CFO: CFO=[60 20 70 10]

The CFO difference of adjacent users: delta CFO=[40 -50 60 -50],

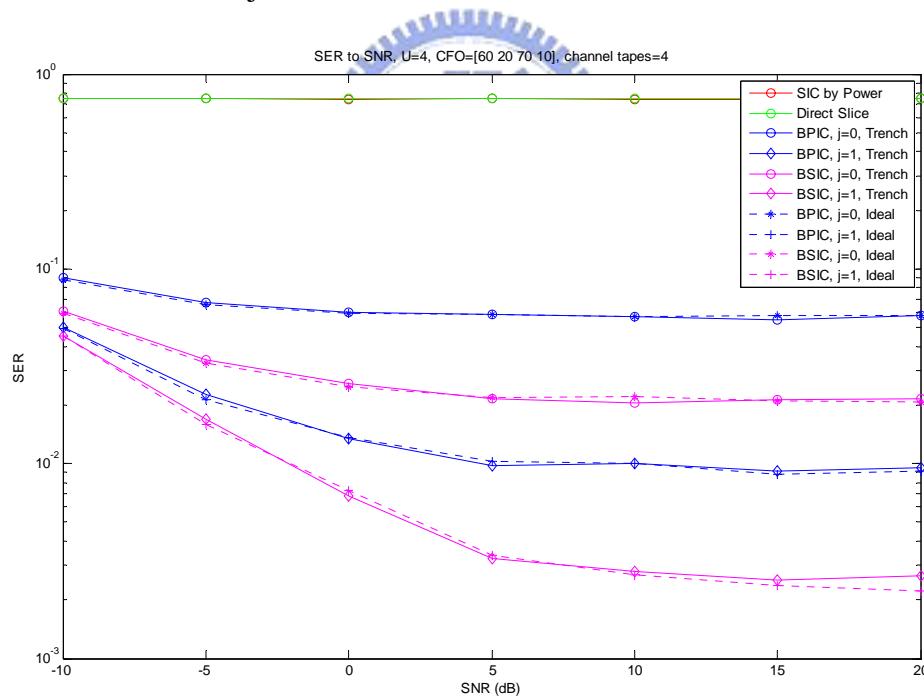


Figure 4.2.2.1 Comparison Trench algorithm and ideal inversion, Symbol Error Rate to SNR (dB) sets, U=8, CFO=[40 -50 60 -50], Rayleigh fading channel tapes=4

The dotted lines are the results of ideal inversion, and the solid lines are the results of the Trench algorithm.

B. Number of subscriber:8

Subscriber's CFO: CFO=[40 20 70 10 65 25 75 15]

The difference with adjacent users: delta CFO=[20 -50 60 -55 40 -50 60 -25]

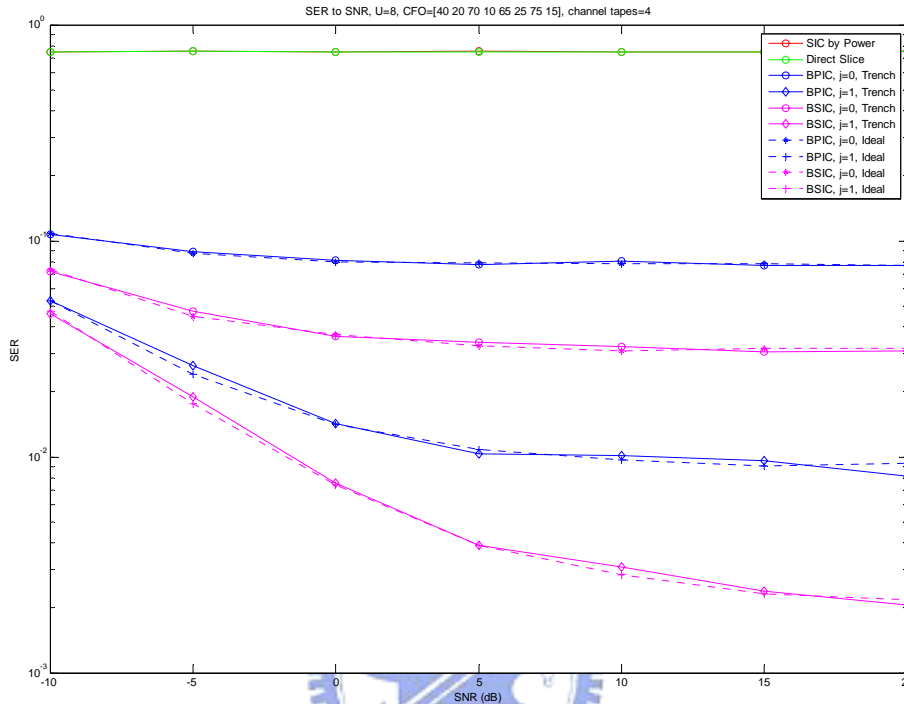


Figure 4.2.2.2 Comparison Trench algorithm and ideal inversion, Symbol Error Rate to SNR (dB) sets, U=8, CFO=[20 -50 60 -55 40 -50 60 -25], Rayleigh fading channel tapes=4

In the figure 4.2.2.2 the solid line are the result of Trench algorithm, and the dotted lines are result of ideal inversion computation.

Not matter in the case A or in the case B does the trench algorithm perform as good as the ideal inversion. The Trench algorithm requires less computation than the ordinary matrix inversion computation. For example, in the case B, it takes $O(3 \cdot n^2)$, $n=8$, to compute a submatrix (8 by 8). Hence, the Trench algorithm is very suitable for digital circuit realization [25].

4.2.3. Multistage Iteration

The BPIC and BSIC schemes are the multistage detectors. They can iteratively reconstruct and cancel the interference from the signals. In order to observe how the performance is improved by increasing the number of iterations, we conduct the simulation with three iterations. The result of the third stage is marked with index, $j=2$.

The conditions are the same as those in section 4.2.2. The number of subscribers is 4. The CFO set is [60 20 70 10].

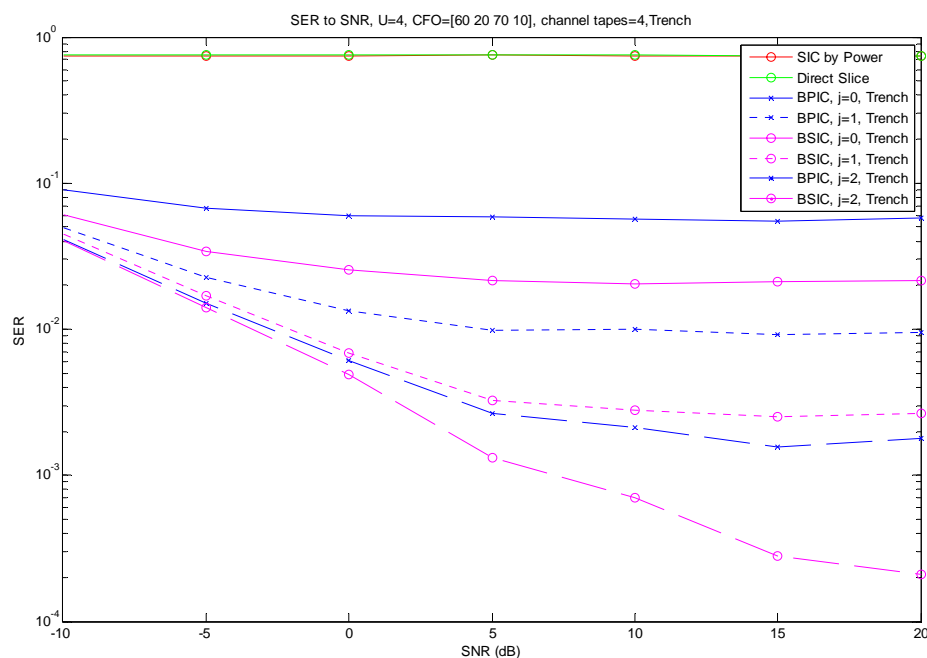


Figure 4.2.3 Performance of iteration in second stage, Symbol Error Rate to SNR, $U=4$, CFO=[60 20 70 10], Rayleigh fading channel, tapes=4.

In figure 4.2.3, the solid lines mean the results with a single iteration, the dotted lines represent the results with two iterations, and the dashed lines are the results with three iterations (the results of the third stage).

We can see that when SNR is 20 dB, the performance would be 10 times better than the last iteration for both the BPIC and the BSIC schemes. The BSIC scheme outperforms the BPIC scheme.

5. Conclusion and Future Work

5.1. Conclusion

In this thesis, we propose two block based CFO interference cancellation (IC) schemes: Block Parallel Interference Cancellation (BPIC) and Block Serial Interference Cancellation (BSIC). Both schemes are able to be iteratively processed to achieve target performance. Instead of solving the Carrier Frequency Offsets (CFOs) problem in time domain, both of them compensate and eliminate the influence caused by CFOs in frequency domain.

In the comparison between the BPIC scheme and the BSIC scheme, though the BSIC scheme requires more time to iterate the cancellation than the BPIC scheme, the BSIC scheme can provide good performance. The reason is that the first iteration of the BSIC can provide more reliable symbol detection than that of the BPIC scheme. The performance comparison of the different algorithms is made by using the computer simulation in chapter 4.

To save the computation complexity required for Toeplitz matrix inversion, the Trench algorithm, which only takes $O(3n^2)$ computation, is applied in the proposed algorithms. This makes the implement of the BSIC scheme and the BPIC scheme possible for the digital circuit design.

5.2. Future Work

At the end of this thesis, I summarize some directions for the future research about OFDMA.

The Frequency Hopping (FH) technique can be employed into OFDMA systems to achieve frequency diversity. Our proposed schemes are based on the block-wise. The study of block-wise FH of the OFDMA system may be an interesting topic. It is possible to apply the FH technique into the BPIC and BSIC schemes and to randomize the ICI with a proper hopping pattern.

The estimation of the CSI and the CFOs is always the most important issue of the OFDMA system. There is no guarantee on the good performance unless good estimation of the CSI and the CFO is made. In this way, timing synchronization and channel estimation are tasks to the proposed system



6. Reference:

- [1] H. Rohling and R. Grunheid, "Performance of an OFDM-TDMA mobile communication system," in *Proceedings of the IEEE Semiannual Vehicular Technology Conference*, 46th, May 1996, pp. 1589–1593.
- [2] J. Choi, C. Lee, H. W. Jung, and Y. H. Lee, "Carrier frequency offset compensation for uplink of OFDM-FDMA systems," *IEEE Commun. Lett.*, vol. 4, no. 12, pp. 414–416, December 2000.
- [3] S. Hara and R. Prasad, "Overview of multicarrier CDMA," *IEEE Commun. Mag.*, vol. 35, no. 12, pp. 126–133, Dec. 1997.
- [4] D. Kivanc, G. Li, and H. Liu, "Computationally efficient bandwidth allocation and power control for OFDMA," *IEEE Trans. Wireless Commun.*, vol. 2, no. 6, pp. 1150–1158, Nov. 2003.
- [5] A. M. Tonello, N. Laurenti, and S. Pupolin, "Analysis of the uplink of an asynchronous multi-user DMT OFDMA system impaired by time offsets, frequency offsets, and multi-path fading," in *VTC Conference Record*, vol. 3, October 2000 Fall, pp. 1094–1099.
- [6] Z. Gao, U. Tureli and Y. D. Yao, "Deterministic multiuser carrierfrequency offset estimation for interleaved OFDMA uplink," *IEEE Trans. Commun.*, vol. 52, pp. 1585– 1594, Sep. 2004.
- [7] Man-On Pun, Shang-Ho Tsai, Kuo, C.-C.J., "Joint maximum likelihood estimation of carrier frequency offset and channel in uplink OFDMA systems," in *GLOBECOM 2004, IEEE*, vol. 6, pp. 3748– 3752.
- [8] L. Kuang, J. Lu, Z. Ni, J. Zheng, "Nonpilot-aided carrier frequency tracking for uplink OFDMA systems," in *ICC 2004, IEEE*, vol. 6, pp. 3193– 3196.
- [9] J.A.C.Bingham, "Multicarrier Modulation for Data Transmission: An Idea Whose Time Has Come " Vol 28, Issue 5, May 1990 Page(s):5 - 14
- [10] I. K. Fu, "A Dynamic Simulation Platform for Heterogeneous multiple Access Systems," Thesis of Master Degree, National Chung Cheng University, 2002.
- [11] Y. Zhao and S.-G. Haggman, "Sensitivity to Doppler shift and carrier frequency errors in OFDM systems-The consequence and solutions," in *IEEE 64th Vehicular Technology Conf*, Atlanta, GA, Apr.1996, pp.1564-1568.
- [12] S. B. Weinstein and P. M. Ebert, "Data transmission by frequency-division multiplexing using the discrete Fourier transform," *IEEE Trans. Commun. Technol.*, vol. COM-19, pp.628-634, Oct. 1971.
- [13] M. Gudmundson and P.-O. Aderson, "Adjacent channel interference in an OFDM system," in *IEEE 46th Vehicular Technology Conf.*, Atlanta, GA, Apr. 1996, pp.918-922.

- [14] M. Gudmundson and P.-O. Anderson, "Adjacent channel interference in an OFDM system," in IEEE 64th Vehicular technology Conf., Atlanta, GA, Apr. 1996, pp.918-922.
- [15] C. Muschallik, "Improving an OFDM reception using an adaptive Nyquist windowing," IEEE Trans. Consumer Electron, vol.42, Aug. 1996.
- [16] D. Verhulst, M. Mouly, and J. Szpirglas, "Slow frequency hopping multiple access for digital cellular radiotelephone," IEEE J, Select. Areas Commun., vol. 2, pp. 563-574, July 1984
- [17] H. Olofsson, J.. Naslund, and J. Skold, "Interference diversity gain in frequency hopping GSM," in Proc. VTC. Vol. 1, Aug. 1995, pp. 102-106
- [18] G. J. Pottie and A. R. Calderbank, "Channel coding strategies for cellular radio," IEEE Trans. Veh. Technol., vol. 44 pp. 763-770, Nov. 1995.
- [19] Jianfeng QIANG and Ping ZHANG, "Filter Bank Based Multiuser Receiver for Wireless OFDMA System" IEEE 2005
- [20] Tonello A.M, Laurenti N., Pupolin S., "Analysis of the uplink of an asynchronous multi-user DMT OFDMA system impaired by time offsets, frequency offset, and multipath fading," Vehicular Technology Conference, 2000. IEEE VTS-Fall VTC 2000. 52nd., Volumn:3.24-28 Sept. 2000 Pages:1094-1099 vol.3.
- [21] Zhongren Cao, Ufuk Tureli, Yu-Dong Yao and Patrick Honan., "Frequency Synchronization for Generalized OFDMA Uplink" IEEE commun 2004 pp.1071-1075
- [22] J.J. Van de Beek, P.O.Borjesson, D. Landstram, J.M. Areans, P.Odling, C. Ostberg, M. Wahlqvist, S. K. Wilson, "A time and frequency synchronization scheme for OFDMA," IEEE J. Select. Area Commun., vol. 17 pp.1900-1914, Nov.1999.
- [23] R. Fantacci, D. Marabissi, S. papini, "Multiuser Interference Cancellation Receiver for OFDMA Uplink Communications with Carrier Frequency offset," IEEE Commun 2004 pp.2808-2812
- [24] Sergio Verdu, "Multituser Detection," Cambridge University Press
- [25] Shalhav Zohor, "Toeplitz Matrix Inversion: The Algorithm of W.F. Trench," Journal of the Association for Computing machinery, Vol. 16, No.4, October 1969, pp.592-601